Article:
Weigert, S. (1993) Quantum chaos in the configurational quantum cat map. Physical Review A. pp. 1780-1798. ISSN: 1094-1622

https://doi.org/10.1103/PhysRevA.48.1780

Quantum chaos in the configurational quantum cat map

Stefan Weigert
Institut für Physik, Klingelbergstrasse 82, CH-4056 Basel, Switzerland
(Received 4 March 1993)

The motion of a classical or quantum-mechanical charged particle in the unit square (with periodic boundary conditions) is investigated under the influence of periodic electromagnetic fields. It is shown that the external fields can be chosen in such a way that the configuration space of the particle is mapped periodically to itself according to Arnold's cat map. The time evolution of the quantum system shows the same degree of irregularity as does the classical time evolution which is completely dominated by the properties of the hyperbolic map. In particular, the eigenfunctions of the Floquet operator are determined analytically, and, as an immediate consequence, the spectrum of quasienergies in this system is seen to be absolutely continuous. Furthermore, spatial correlations decay exponentially. The observed features are in striking similarity to properties of classically chaotic systems; for example, long-time predictions of the future behavior of the system turn out to be extremely sensitive to the specification of the initial state. In other words, the time evolution of the quantum system is algorithmically complex. These phenomena, based on the formation of arbitrarily fine structures in the two-dimensional configuration space, require that the system absorb energy (provided by the external kicks) at an exponential rate.

PACS number(s): 03.65.−w, 03.20.+i

I. INTRODUCTION

The time evolution of a quantum-mechanical system is, in general, governed by two mutually exclusive processes. On the one hand, there is the deterministic transformation of a wave function at time t into another wave function at time t' according to Schrödinger's equation. On the other hand, there is the process of measurement which introduces an unpredictable interaction of the "classical apparatus" with the microscopic quantum system.

One aspect of interest in the context of "quantum chaos" (see, e.g., [1] or [2]) is the question of whether the deterministic time evolution of simple quantum systems may exhibit familiar features from the behavior of classically chaotic Hamiltonian systems [3]. More specifically, one asks whether the time evolution of wave functions generated by a "natural" Hamilton operator shows truly chaotic behavior or "deterministic randomness" [4], i.e., phenomena such as ergodicity, mixing, or being Bernoulli. The occurrence of these phenomena in generic classical systems has far-reaching *physical* consequences: the long-time behavior of such systems becomes effectively inaccessible. Note that these considerations completely focus on the deterministic time evolution of the wave function [5]. Under the assumption that quantum mechanics actually is the fundamental theory which contains classical mechanics as a limit (see, however, [6]) answers to these questions will have some impact on the foundations of quantum statistical mechanics.

In the present work it will be shown for a particular model that the quantum-mechanical time evolution can be deterministically random, despite the "linearity" of Schrödinger's equation with respect to the wave function. Consequently, in this quantum-mechanical model (and presumably a whole class of similar systems) one faces the problem of extremely difficult long-time predictions. Before presenting the actual model system and its detailed investigation, the motivation for its choice and the underlying physics will be discussed in general terms.

In classical mechanics time-dependent Hamiltonian systems and, closely related, area-preserving maps represent important models: observing a system at discrete times only is sufficient to reveal those features which are characteristic of chaotic motion. Such abstractions from the actual smooth phase-space dynamics clearly have the advantage to bring into focus the important traits. For example, the simple dynamics of the baker transformation [3] is rich enough to generate orbits with a high degree of irregularity while, at the same time, the time evolution is partly amenable to analytical investigation.

To some extent, the search for irregular behavior in quantum-mechanical systems relies on quantized versions of one-dimensional time-dependent Hamiltonian systems, e.g., the "quantum standard map" [7] or the "kicked spin" [8]. The motivation for a study of such systems is given by the fact that the discrete energy spectrum in autonomous bounded quantum systems necessarily leads to quasiperiodic (and therefore simple) time evolution of wave functions and expectation values [9,10]. The investigation of time-dependent systems, in contrast, is principally promising because the time-evolution operator *may* have a continuous spectrum of quasienergies which would allow us to draw parallels with classically chaotic motion. Various properties of such systems have been determined numerically and have led to unforeseen misfits of the classical and quantum-mechanical dynamics [11]. The subtleties of the quasienergy spectrum, however, make analytic results highly desirable (see examples in

[12,13]).

Linear hyperbolic maps of the unit square to itself are among the simplest examples of chaos-generating maps, Arnold's cat map [14] being a prominent example. Berry *et al.* [15] and Ford, Mantica, and Ristow [16] present ways to introduce such maps as an element of the time evolution of a quantum system. They consider the unit square as the phase space of a classical system with one degree of freedom. The state of the system at time $t=T_n\equiv nT\geq 0$ ($n=0,1,2,\ldots$) is determined by the n-fold application of a linear hyperbolic map on the initial conditions (x_0,p_0). The underlying dynamics is Hamiltonian so that quantization can be effected, e.g., by construction of the quantum propagator $U(x',x)$. Hence the implementation of a hyperbolic map into the quantum-mechanical time evolution has been achieved. It turns out that the inevitably coarse-grained structure of the two-dimensional "quantum phase space" does not allow the formation of those phase-space structures which, typically, are associated with chaotic systems.

In the following it is demonstrated that this difficulty can be by-passed by investigating physical systems with more than one degree of freedom which classically show "configurational chaos." This means that the knowledge of the motion in the configuration space alone is sufficient to recognize the chaotic behavior of trajectories in the full phase space.

In order to investigate consequences of classical configurational chaos in quantum systems, a time-periodic physical system with two degrees of freedom is presented [17] which classically and quantum mechanically can be studied extensively by analytic means. A linear hyperbolic map is built into the Hamiltonian time evolution in a way different from the approaches by Berry *et al.* and Ford, Mantica, and Ristow which does not suppress the occurrence of irregular motion. Related work was done by Chirikov, Izrailev, and Shepelyansky [18], who in this context coined the notion of "true quantum chaos." These authors analyzed an abstract autonomous model with at least three degrees of freedom, and they showed that there are indeed features of configurational chaos which survive quantization (cf. also [19]).

Consider the unit square not as *phase* space of a fictitious physical system with one degree of freedom but as *configuration* space of a system with *two* degrees of freedom. Then, a linear hyperbolic map of the unit square onto itself can be regarded as part of a canonical point transformation in the four-dimensional phase space, and the transformation of the conjugate momenta is determined by the transformation of coordinates. Physically the associated Hamiltonian describes a charged particle which, under the influence of external electromagnetic fields, moves in the unit square with periodic boundary conditions. In other words, the configuration space has the topology of a two-dimensional torus and the particle can wind around the torus with arbitrary velocity, implying that the phase space is unbounded in momentum direction. The Hamiltonian description of the system allows one to define a quantum analog in a straightforward way.

In comparison to the one-dimensional models mentioned earlier, two differences stand out. First, the momenta are *not* bounded; second, the hyperbolic map in this model is applied to pairs of variables the operator counterparts of which *do* commute. This property will turn out to be crucial: as a consequence the quantum time evolution in the coordinate basis largely parallels the classical configurational chaos. In principle, arbitrarily fine structures may develop in configuration space, simply because the position operators commute. For instance, the process of "stretching and folding" the configuration space of the classical system is reflected in an analogous transformation of the position basis of the quantum system. A necessary prerequisite for this phenomenon is the unboundedness of the classical phase space. However, it is important to emphasize the following point: in contrast to classical dynamics the knowledge of the "configurational time evolution" alone (corresponding to the history of the position basis) already represents the *maximal* information one can have about the state of the quantum system, and it is completely legitimate to restrict one's attention to the time evolution of the configuration-space basis.

The paper is divided into four parts. In Sec. II the model is defined, the time evolution of its classical version is presented, and the algorithmic complexity of its orbits is determined. Then, in Sec. III, the Floquet operator of the associated quantum system is studied. Its exact eigenfunctions and the quasienergy spectrum are determined. The quantum-mechanical time evolution of states for the case of a "quantum resonance" turns out to be particularly simple as it is shown in Sec. IV. Furthermore, the time evolution of several expectation values, variances, and correlation functions is determined. "Quantum orbits" turn out to be extremely irregular if, in a natural way, the concepts "Bernoulli shift," complexity," and "sensitive dependence on initial conditions" are applied to the quantum model. In Sec. V, the results are discussed and a summary is given.

II. THE CLASSICAL SYSTEM

A. The Hamiltonian

The system to be studied is defined by the Hamiltonian

$$H(\mathbf{x},\mathbf{p},t)=\tfrac{1}{2}\tilde{\mathbf{p}}\cdot\mathbf{p}+\tilde{\mathbf{p}}\cdot\mathbf{F}(\mathbf{x},t)\ , \tag{1}$$

where $\tilde{\mathbf{p}}$ denotes the transpose of $\mathbf{p}$. It describes a charged particle of mass $m=1$ constrained to move in a unit square of the xy plane with periodic boundary conditions (period 1). The canonically conjugate variables $\mathbf{x}$ and $\mathbf{p}$ satisfy the Poisson-bracket relations $\{\mathbf{x},\mathbf{p}\}=\mathbf{1}_2$ where $\mathbf{1}_2$ is the 2×2 unit matrix and $\mathbf{F}(\mathbf{x},t)$ is an explicitly time-dependent vector field in the plane of motion [the notations $\mathbf{x}\equiv(x,y)\equiv(x_1,x_2)$ are used interchangeably throughout]. The physical interpretation of the Hamiltonian $H(\mathbf{x},\mathbf{p},t)$ results from writing (1) in the form

$$H'(\mathbf{x},\mathbf{p},t)=\frac{1}{2}\left[\tilde{\mathbf{p}}-\frac{e}{c}\,\tilde{\mathbf{A}}(\mathbf{x},t)\right]\cdot\left[\mathbf{p}-\frac{e}{c}\,\mathbf{A}(\mathbf{x},t)\right]+e\phi(\mathbf{x},t)\ . \tag{2}$$

As functions of the field $\mathbf{F}(\mathbf{x},t)$ the vector potential $\mathbf{A}(\mathbf{x},t)$ and the scalar potential $\phi(x,t)$ read

$$\mathbf{A}(\mathbf{x},t)=-\frac{c}{e}\mathbf{F}^{(-)}(\mathbf{x},t)\ ,$$
$$\phi(\mathbf{x},t)=\frac{1}{2e}\tilde{\mathbf{F}}(\mathbf{x},t)\cdot\mathbf{F}(\mathbf{x},t)-\frac{1}{c}\frac{\partial f(\mathbf{x},t)}{\partial t}\ . \tag{3}$$

The prime in Eq. (2) indicates that the rotation-free part $\mathbf{F}^{(+)}=(e/c)\nabla f(\mathbf{x},t)$ of the decomposed vector field $\mathbf{F}=\mathbf{F}^{(-)}+\mathbf{F}^{(+)}$ has been removed from the vector potential $\mathbf{A}(\mathbf{x},t)$ by a gauge transformation. The electric field

$$\mathbf{E}(\mathbf{x},t)=-\nabla\phi(\mathbf{x},t) \tag{4}$$

associated with Eq. (1) has components in the xy plane only whereas the magnetic field

$$\mathbf{B}(\mathbf{x},t)=\nabla\times\mathbf{A}(\mathbf{x},t) \tag{5}$$

is directed along the z axis.

For the following it is sufficient to restrict one's attention to a linear and time-periodic vector field

$$\mathbf{F}(\mathbf{x},t)=\mathbf{V}\cdot\mathbf{x}\Delta_{T,\epsilon}(t)\equiv(\mathbf{V}^{(+)}+\mathbf{V}^{(-)})\cdot\mathbf{x}\Delta_{T,\epsilon}(t)\ . \tag{6}$$

Here $\Delta_{T,\epsilon}(t)$ is a sequence of smooth kicks of period T, duration $\propto\epsilon$, and height $\propto 1/\epsilon$ ($\epsilon\ll T$). Each of the kicks is normalized

$$\int_{-\epsilon}^{+\epsilon}\Delta_{T,\epsilon}(t)dt=1\ , \tag{7}$$

and in the limit $\epsilon\to 0$ one recovers a periodic δ function

$$\lim_{\epsilon\to 0}\Delta_{T,\epsilon}(t)=\delta_T(t)\equiv\sum_{n=-\infty}^{\infty}\delta(t-nT)\ . \tag{8}$$

The constant 2×2 matrix $\mathbf{V}$ has the property that $\mathbf{M}=\exp[\mathbf{V}]$ is a hyperbolic matrix with integer entries only and its determinant is equal to unity.

In this case during a kick there acts an electric field

$$\mathbf{E}(\mathbf{x},t)=\left[-\Delta_{T,\epsilon}^2(t)\tilde{\mathbf{V}}\cdot\mathbf{V}+\frac{\partial\Delta_{T,\epsilon}(t)}{\partial t}\mathbf{V}^{(+)}\right]\cdot\mathbf{x} \tag{9}$$

and the magnetic field is given by

$$\mathbf{B}(\mathbf{x},t)=-\frac{c}{e}\Delta_{T,\epsilon}(t)(V_{yx}-V_{xy})\mathbf{e}_z\ . \tag{10}$$

A symmetric matrix $\mathbf{V}\equiv\mathbf{V}^{(+)}$ corresponds to a symmetric hyperbolic map $\mathbf{M}$ and leads to

$$H'(\mathbf{x},\mathbf{p},t)=\frac{1}{2}\tilde{\mathbf{p}}\cdot\mathbf{p}-\frac{1}{2e}\tilde{\mathbf{x}}\cdot\mathbf{\Omega}(t)\cdot\mathbf{x}\ . \tag{11}$$

Formally, this is a harmonic oscillator with a time-dependent frequency matrix $\mathbf{\Omega}(t)$. It should be noted that in $\mathbf{\Omega}(t)$ the square and the derivative of the kick function $\Delta(t)$ are present.

Contrary to well-known and thoroughly studied one-dimensional kicked models, in this system the amplitude of the kicks depends on the *phase* (i.e., position and momentum) of the system, not on the configuration alone. The consequence of the familiar *spatial* dependence is a discontinuous behavior of the momenta as a function of time—the $\mathbf{p}$ dependence in addition will lead to discontinuous behavior of the coordinates. (As long as $\epsilon>0$, however, all quantities change continuously in time. Only for mathematical convenience is the limit $\epsilon\to 0$ taken later on.) Note that the amplitude of the kick in the gauge-transformed Hamiltonian H' no longer depends on the momentum $\mathbf{p}$ if $\mathbf{V}$ is chosen to be a symmetric matrix $\mathbf{V}^{(+)}$. In this case the discontinuity in the momenta is hidden in the specific time dependence of the kicking potential: in particular, it is due to the presence of the derivative of the kick function $\Delta(t)$.

B. The time evolution

How does the classical system evolve in the course of time, given the initial conditions $\mathbf{x}(t_0)$ and $\mathbf{p}(t_0)$? The equations of motion follow from the Hamiltonian $H(\mathbf{p},\mathbf{x})$ as

$$\begin{aligned}\dot{\mathbf{x}}&=\{H,\mathbf{x}\}=\mathbf{p}+\mathbf{V}\cdot\mathbf{x}\Delta_{T,\epsilon}(t)\ ,\\ \dot{\mathbf{p}}&=\{H,\mathbf{p}\}=-\tilde{\mathbf{V}}\cdot\mathbf{p}\Delta_{T,\epsilon}(t)\ .\end{aligned} \tag{12}$$

Two components of the dynamics are to be distinguished: the free time evolution for times $T_n+\epsilon<t<T_{n+1}-\epsilon$ and the kick dynamics during the intervals $T_n-\epsilon<t<T_n+\epsilon$, $n\in\mathbb{Z}$. During the free time evolution both components of the momentum are conserved. Hence the particle moves with constant velocity along a straight line. Subsequently, the equations of motion relate the coordinates $\mathbf{x}^-$ and momenta $\mathbf{p}^-$ immediately before the kick time T_0 to the set $(\mathbf{x}^+,\mathbf{p}^+)$ immediately after the time T_0. Here one may pick with full generality the kick at $t=T_0\equiv 0$ because of the periodicity of the Hamiltonian: $H(t)=H(t+nT), n\in\mathbb{Z}$. The time dependence of the momenta for times $-\epsilon\le t\le+\epsilon$ follows directly from integrating Eq. (12)

$$\mathbf{p}(t)=e^{-\tilde{\mathbf{V}}\Theta_\epsilon(t)}\cdot\mathbf{p}(-\epsilon),\quad |t|\le\epsilon\ , \tag{13}$$

where

$$\Theta_\epsilon(t)=\int_{-\epsilon}^{t}\Delta_{T,\epsilon}(t')dt' \tag{14}$$

is a smooth version of the step function with $\Theta_\epsilon(-\epsilon)=0$ and $\Theta_\epsilon(\epsilon)=1$. The continuous evolution in (13) shows that the momenta have finite values for all times and arbitrary ϵ. In the limit of arbitrarily small ϵ the relation between the momenta before and after the kick, $\mathbf{p}^-$ and $\mathbf{p}^+$, becomes

$$\lim_{\epsilon\to 0}\mathbf{p}(\epsilon)=\mathbf{p}^+=e^{-\tilde{\mathbf{V}}}\cdot\mathbf{p}^-\equiv\tilde{\mathbf{M}}^{-1}\cdot\mathbf{p}^-\ , \tag{15}$$

where $V=\ln\mathbf{M}$.

Along the same lines one can derive the effect of the kick on the coordinates in the limit $\epsilon\to 0$. Making use of the finiteness of the momenta during the kick one finds

$$\lim_{\epsilon\to 0}\mathbf{x}(\epsilon)=\mathbf{x}^+=e^{\mathbf{V}}\cdot\mathbf{x}^-\equiv\mathbf{M}\cdot\mathbf{x}^-\ , \tag{16}$$

so that the total transformation $(\mathbf{x}^-,\mathbf{p}^-)\to(\mathbf{x}^+,\mathbf{p}^+)$ is manifestly canonical. In this equation it is understood that the unit square is mapped onto itself; strictly speaking, a mod1 prescription should appear on the right-hand side. As a result, the Hamiltonian $H(\mathbf{p},\mathbf{x},t)$ entails equa-

tions of motion with hyperbolic maps (acting separately on coordinates and momenta) built into the time evolution.

It is noteworthy that the canonical momenta $\mathbf{p}$ and the *velocity* $\mathbf{v}$

$$v_x(t)\equiv\frac{dx(t)}{dt}=\lim_{\epsilon\to\infty}\frac{x(+\epsilon)-x(-\epsilon)}{2\epsilon}\sim\lim_{\epsilon\to 0}\frac{1}{2\epsilon}=\infty \quad (17)$$

behave in a qualitatively different way. From the relation

$$\mathbf{v}(t)=\mathbf{p}(t)-\frac{e}{c}\mathbf{A}(\mathbf{x},t) \quad (18)$$

it is clear that $\mathbf{v}$ contains contributions of the vector potential $\mathbf{A}(\mathbf{x},t)$ which, in the limit $\epsilon\to 0$, become arbitrarily large.

What do typical trajectories look like in phase space? The trajectory of a particle positioned at $\mathbf{x}(t_0)\equiv\mathbf{x}_0$ with zero momentum $\mathbf{p}(t_0)\equiv\mathbf{p}_0=0$ is easily visualized: there is no motion of the particle in phase space except at times T_n, $n\in\mathbb{Z}$. At these times, however, it is moved instantaneously by the application of combined electric and magnetic fields to a new position

$$\mathbf{x}_n(t_0)=(\mathbf{M}^n\cdot\mathbf{x}_0)\mathrm{mod}1,\quad n\in\mathbb{N} \quad (19)$$

with zero momentum again. Thus the orbit can be calculated by repeated application of the hyperbolic map $\mathbf{M}$ to the coordinates and consists of a sequence of isolated points in phase space. The phase-space trajectory of a particle with nonvanishing initial momentum $\mathbf{p}_0$ is composed of an infinite number of disconnected straight lines instead of points.

If the initial momenta $\mathbf{p}_0$ fulfill the relation

$$\mathbf{p}_0T=\mathbf{n},\quad n_x,n_y\in\mathbb{Z}\ , \quad (20)$$

the motion is called resonant. Starting at $\mathbf{x}_0$ at time T_0^+, the particle returns exactly to this point at time T_1^-. In this particular case, under stroboscopical observation of the time evolution in configuration space, there is no difference between this trajectory and another one generated by a particle initially resting at $\mathbf{x}_0$.

One can write down a formal solution of the equations of motion, Eqs. (12), for arbitrary initial conditions $\mathbf{x}_0$ and $\mathbf{p}_0$. Let $\bar{t}_0=T-t_0$ be the time from t_0 up to the first kick, which will be chosen to be at $t=T_1$. Then one has in the time interval $T_n<t<T_{n+1}$, $n\in\mathbb{N}$,

$$\begin{aligned}\mathbf{x}(t)=\mathbf{M}\cdot(\cdots\{[M\cdot(\mathbf{x}_0+\mathbf{p}_0\bar{t})\mathrm{mod}1\\ +\tilde{\mathbf{M}}^{-1}\cdot\mathbf{p}_0T]\mathrm{mod}1+\cdots\}\cdots\\ +\tilde{\mathbf{M}}^{-n}\cdot\mathbf{p}_0t)\mathrm{mod}1\ ,\\ \mathbf{p}(t)=\tilde{\mathbf{M}}^{-1}\cdot\mathbf{p}_0\ .\end{aligned} \quad (21)$$

Although these expressions are explicit, it is extremely complicated to predict the long-time behavior of solutions. Trajectories, initially close together, will quickly be separated by the stretching mechanism contained in the hyperbolic maps $\mathbf{M}$ and $\tilde{\mathbf{M}}^{-1}$, requiring a high accuracy of the initial conditions for valuable forecasts. This can be seen from a calculation of the associated Lyapunov exponents which are a measure of the divergence of initially close trajectories [3]: What is the image $\delta\mathbf{z}(t_0+T)$ of a vector

$$\delta\mathbf{z}(t_0)\equiv(\delta\mathbf{x}(t_0),\delta\mathbf{p}(t_0))\equiv(\mathbf{x}_2(t_0)-\mathbf{x}_1(t_0),\mathbf{p}_2(t_0)-\mathbf{p}_1(t_0)) \quad (22)$$

after one period T? An approximate answer can be found from a linearized version of the mapping (21)

$$\delta\mathbf{z}(t_0+T)=\mathcal{M}\cdot\delta\mathbf{z}(t_0)\ , \quad (23)$$

where the 4×4 matrix $\mathcal{M}$ turns out to be

$$\mathcal{M}=\begin{bmatrix}\mathbf{M} & \bar{t}_0\mathbf{M}+(T-\bar{t}_0)\tilde{\mathbf{M}}^{-1}\\ 0 & \tilde{\mathbf{M}}^{-1}\end{bmatrix}\equiv\begin{bmatrix}\mathbf{M} & \mathbf{m}(t_0)\\ 0 & \tilde{\mathbf{M}}^{-1}\end{bmatrix}\ . \quad (24)$$

Having determinant 1 the matrix $\mathbf{M}$ is "volume conserving" in configuration space. For simplicity it is assumed to be symmetric from now on. Arnold's cat map [14] is effected by

$$\mathbf{C}=\begin{bmatrix}2 & 1\\ 1 & 1\end{bmatrix}\ , \quad (25)$$

representing a well-known example of such a matrix. There is an orthogonal 2×2 matrix $\mathbf{D}$ which brings $\mathbf{M}$ to diagonal form

$$\tilde{\mathbf{D}}\cdot\mathbf{M}\cdot\mathbf{D}=\mathbf{\Lambda}=\begin{bmatrix}\lambda & 0\\ 0 & 1/\lambda\end{bmatrix},\quad \lambda\in\mathbb{R}_+/\{1\}\ . \quad (26)$$

The structure of the eigenvalues λ and $1/\lambda$ is generic for hyperbolic maps.

Applying the matrix

$$\mathcal{D}=\begin{bmatrix}\mathbf{D} & 0\\ 0 & \mathbf{D}\end{bmatrix} \quad (27)$$

to Eq. (23) one obtains

$$\delta\mathbf{z}'(t_0+T)=\tilde{\mathcal{D}}\cdot\mathcal{M}\cdot\mathcal{D}\delta\mathbf{z}'(t_0)\equiv\mathcal{M}'\delta\mathbf{z}'(t_0)\ , \quad (28)$$

where $\delta\mathbf{z}'\equiv\mathcal{D}\cdot\delta\mathbf{z}$. Then the Lyapunov exponents of map (21) are given by the logarithms of the eigenvalues of the linearized map

$$\mathcal{M}'=\begin{bmatrix}\mathbf{\Lambda} & \tilde{\mathbf{D}}\cdot\mathbf{m}(t_0)\cdot\mathbf{D}\\ 0 & \mathbf{\Lambda}^{-1}\end{bmatrix}\ . \quad (29)$$

Truly chaotic behavior, however, is associated only with motion in a bounded volume of phase space. Consequently, it is not appropriate to infer possible irregular behavior of the system from the full matrix $\mathcal{M}'$. Instead, a study of the configurational motion alone is reasonable because in configuration space the motion is bounded. Assume, for simplicity, that the initial momentum is equal to zero. Then one finds

$$\delta\mathbf{x}'(t_0+T)=\mathbf{\Lambda}\delta\mathbf{x}'(t_0)\ , \quad (30)$$

and the "configurational Lyapunov exponents" are given by

$$\lambda^{\pm}=\pm|\ln\lambda|\ . \quad (31)$$

They determine the rate of "stretching and folding" along the eigendirections of the matrix $\mathbf{C}$—not in phase space but in configuration space. Taking nonvanishing momenta into account, one also obtains in addition some imaginary contribution to the Lyapunov exponent due to the regular motion along a straight line in between the kicks.

Knowing the time evolution of the basic variables $\mathbf{x}(t)$ and $\mathbf{p}(t)$ the time development of any other phase-space function can be derived. Consider, for instance, the energy $H(\mathbf{x},\mathbf{p},t)$. Obviously, it is not a constant of motion: its value changes at the kick times T_n. In between any two kicks at T_n and T_{n+1} it has a constant value which is related to the Lyapunov exponents of the map $\mathbf{M}$ according to

$$H(\mathbf{x},\mathbf{p},t)=\tfrac{1}{2}\tilde{\mathbf{p}}(t)\cdot\mathbf{p}(t)=\tfrac{1}{2}\tilde{\mathbf{p}}_0\cdot\tilde{\mathbf{D}}\cdot\mathbf{M}^{2n}\cdot\mathbf{D}\cdot\mathbf{p}_0$$
$$=\tfrac{1}{2}(e^{n|\ln\lambda^2|}p'^2_{x,0}+e^{-n|\ln\lambda^2|}p'^2_{y,0}) \tag{32}$$

for $T_n<t<T_{n+1}$ and $\mathbf{p}'\equiv\mathbf{D}\cdot\mathbf{p}$. Therefore, in general the energy grows exponentially with rate $|\ln\lambda^2|$ and remains constant for all times only if the particle initially is at rest.

From (15), however, the existence of a time-independent constant of motion can be inferred. The momenta before and after a kick are related by

$$\mathbf{p}'^{+}=\mathbf{\Lambda}\cdot\mathbf{p}'^{-}\ . \tag{33}$$

Multiplying these two equations one finds that the quantity

$$p'^{+}_x p'^{+}_y=p'^{-}_x p'^{-}_y \tag{34}$$

does not change its numerical value in the course of time. Hence, for arbitrary times t,t' one has

$$p_x(t)p_y(t)=p_x(t')p_y(t')\ . \tag{35}$$

This relation expresses the fact that all iterated momenta are situated on a (rotated) equilateral hyperbola in momentum space. The product of the components of the momenta p_x and p_y is equal to the area $\mathcal{F}$ of the rectangle defined by parallels to the asymptotes through any point of a hyperbola and the asymptotes. The existence of this constant of motion does not affect the nonintegrability of the system under consideration since for an explicitly time-dependent system with two degrees of freedom *three* invariants are necessary.

C. Complexity of classical orbits

The concept of algorithmic complexity originates from information theory [20–22] and can be used to measure the irregularity of orbits of physical systems. An important example are phase-space trajectories of a system described by classical mechanics. Loosely speaking, the time evolution of a physical system has nonvanishing complexity if the initial conditions of a trajectory—moving in a bounded volume of phase space—have to be given with *exponential* accuracy in order to maintain *constant* numerical accuracy of the predictions for increasing time t. This concept is closely related to the notion of the Lyapunov exponent. Typically—there are exceptions [23]—the algorithmic complexity of trajectories in nonintegrable systems is different from zero [4], whereas trajectories of integrable systems in classical mechanics have vanishing complexity.

The definition of algorithm complexity can be based on the analysis of computer programs designed to generate the orbits of a physical system. Effectively, one is looking for a way to compress as much as possible the information needed for a specification of the orbit. Such a program will, in general, consist of three different parts. (i) There is an algorithm of fixed length N_A (measured in bits) encoding the dynamical laws of the system under consideration. (ii) A certain amount of data is needed in order to specify the initial state of the system. The length $N_D(\Delta,t)$ of this part is not a fixed number: a prescribed accuracy Δ of the output at time t requests $N_D(\Delta,t)$ bits as initial data. (iii) Finally one has to state the time t at which the program should stop requiring roughly $\log_2 t$ bits.

The algorithmic complexity of a classical orbit is then defined as

$$C_{\mathrm{cl}}=\lim_{t\to\infty}\frac{1}{t}[N_A+N_D(\Delta,t)+\log_2 t]\ , \tag{36}$$

where the actual program is assumed to be the *shortest* one existing. It is important to note that in the limit of long times only $N_D(\Delta,t)$ will contribute to the complexity. A linear growth of the inaccuracy with time t is characteristic for integrable systems—the resulting *logarithmic* time dependence of $N_D(\Delta,t)$ on t does not yield positive complexity. In chaotic systems with nonvanishing Lyapunov exponents the exponential growth of errors leads to a *linear* time dependence of $N_D(\Delta,t)$ and therefore to positive complexity.

The orbits described by Eqs. (21) have positive algorithmic complexity—except a set of measure zero corresponding to periodic orbits. The demonstration of this statement can be divided into two steps. (i) Projecting the trajectories of the system on the two-dimensional configuration space one obtains a hyperbolic mapping of the coordinates, which turns out to generate algorithmically complex orbits. (ii) From positive complexity of the "configurational motion" it follows that the full trajectories in the four-dimensional phase space have positive complexity, too.

(i) Neglecting the momenta one can easily visualize a typical path in configuration space. As discussed above there are two elements which determine the time evolution: integrable motion along straight lines between the kicks and a hyperbolic map of the configuration space at the kick times T_n. For $\mathbf{p}=0$ one can identify the time evolution of the system with orbits associated with a hyperbolic map: its "orbits" are defined as the sequence of points in the unit square which result from repeated application of the linear map on an initial point. Hyperbolic maps of the unit square onto itself are Bernoulli systems [24]: it is possible to describe their orbits by the process of shifting the "decimal point" of a real number. One can show that almost all orbits of a Bernoulli system have positive algorithmic complexity. Hence, in the

model investigated here paths which correspond to $\mathbf{p}=0$ indeed have positive algorithm complexity. If $\mathbf{p}\neq 0$, the free motion between the kicks produces an additional linear growth of errors. But this contribution is negligible compared to the effect stemming from the kicks. Consequently, *almost all* configurational paths in this model have algorithmic complexity. If the full continuous time evolution is considered, the integrable motion between the kicks, however, prevents the system of being Bernoulli.

(ii) Projecting a phase-space trajectory to a lower-dimensional manifold can be viewed as retaining in a systematic manner information contained in the original trajectory. Canceling that sequence of the algorithmic part of the program which calculates the retained information or adding a finite sequence to the program which explicitly suppresses particular parts of the output will cause only an irrelevant change of the value of N_A in Eq. (36). Of course the numerical value of the complexity C of the output—if originally different from zero—can be affected by the projection. Its value will *increase* if redundant information is dropped and it will *decrease* if actual information is suppressed—project, for example, all points of an irregular trajectory into the origin. The output clearly has null complexity. Starting from a phase-space trajectory with null complexity it is evident that a projection to configuration space cannot increase its value to a positive value. This would amount to code an irregular orbit in a regular trajectory of complexity zero. Therefore, from positive complexity of a projected orbit one may infer the positive complexity of the original orbit. As a result, the solutions of the equations of motion, Eqs. (21), generically have algorithmic complexity different from zero.

In summary, the classical system defined by the Hamiltonian in Eq. (1) shows a high degree of irregularity in its time evolution although the equations of motion effectively are linear. Linear systems usually possess quantum analogs, the behavior of which is closely related to that of their classical counterparts. It will be demonstrated in the next section that this fact allows one to deal in detail with, for example, the question of "true chaotic behavior" in the time evolution of the system or of the existence of "quantum-mechanical orbits" with positive algorithmic complexity.

III. THE QUANTUM SYSTEM

A. The Heisenberg equations of motion

The quantum version of the Hamiltonian (1) reads

$$\begin{aligned} H(\hat{\mathbf{x}},\hat{\mathbf{p}},t)&=\tfrac{1}{2}\hat{\mathbf{p}}^2+\tfrac{1}{2}[\hat{\mathbf{p}}\cdot\hat{\mathbf{F}}(\mathbf{x},t)+\hat{\mathbf{F}}(\mathbf{x},t)\cdot\hat{\mathbf{p}}] \\ &=\tfrac{1}{2}\hat{\mathbf{p}}^2+\tfrac{1}{2}(\hat{\mathbf{p}}\cdot\mathbf{V}\cdot\hat{\mathbf{x}}+\hat{\mathbf{x}}\cdot\tilde{\mathbf{V}}\cdot\hat{\mathbf{p}})\Delta_{T,\epsilon}(t)\ ; \end{aligned} \tag{37}$$

from now on the tilde on vectors (vector operators) will be suppressed. The symmetrization of the original Hamiltonian guarantees the Hermiticity of the Hamilton operator. The operator analogs $\hat{\mathbf{x}}$ and $\hat{\mathbf{p}}$ of the canonical variables $\mathbf{x}$ and $\mathbf{p}$ are assumed to fulfill the familiar commutation relations. A mathematically rigorous formulation of a charged quantum-mechanical particle moving on a torus under the influence of electromagnetic fields is given in [25].

The equations determining the time evolution of the Heisenberg operators $\hat{\mathbf{x}}$ and $\hat{\mathbf{p}}$ are formally equivalent to the classical equations of motion (12)

$$\begin{aligned} \frac{d\hat{\mathbf{x}}}{dt}&=\frac{i}{\hbar}[\hat{H},\hat{\mathbf{x}}]=\hat{\mathbf{p}}+\mathbf{V}\cdot\hat{\mathbf{x}}\Delta_{T,\epsilon}(t)\ , \\ \frac{d\hat{\mathbf{p}}}{dt}&=\frac{i}{\hbar}[\hat{H},\hat{\mathbf{p}}]=-\mathbf{V}\cdot\hat{\mathbf{p}}\Delta_{T,\epsilon}(t)\ . \end{aligned} \tag{38}$$

In between the kick times T_n these equations simply represent the time evolution of a free quantum-mechanical particle dispersing on the torus.

The effect of the kicks can be determined as in the classical model; one obtains a *linear* relation between the operators $(\hat{\mathbf{x}}^-,\hat{\mathbf{p}}^-)$ directly before and $(\hat{\mathbf{x}}^+,\hat{\mathbf{p}}^+)$ directly after a kick. It is the linearity of the quantum-mechanical equations of motion which allows one to take over all the steps of the calculation performed in the classical case. The time evolution of the coordinate operator $\hat{\mathbf{x}}(t)$ under the influence of the smooth version of a kick $\Delta_{T,\epsilon}(t)$ reads

$$\hat{\mathbf{x}}(t)=e^{\mathbf{V}\Theta_\epsilon(t)}\hat{\mathbf{x}}(-\epsilon),\quad |t|\leq\epsilon\ . \tag{39}$$

Consequently, the kick transformation resulting in the limit of arbitrarily small ϵ turns out to be

$$\begin{aligned} \hat{\mathbf{x}}^+&=e^{\mathbf{V}}\cdot\hat{\mathbf{x}}^-\equiv\mathbf{M}\cdot\hat{\mathbf{x}}^-\ , \\ \hat{\mathbf{p}}^+&=e^{-\tilde{\mathbf{V}}}\cdot\hat{\mathbf{p}}^-\equiv\tilde{\mathbf{M}}^{-1}\cdot\hat{\mathbf{p}}^-\ . \end{aligned} \tag{40}$$

The structure of these equations guarantees that the transformed operators fulfill the canonical commutation relations

$$[\hat{x}_j^+,\hat{p}_k^+]=\sum_{l,m}M_{jl}M_{mk}^{-1}[\hat{x}_l^-,\hat{p}_m^-]=i\hbar\sum_m M_{jm}M_{mk}^{-1}=i\hbar\delta_{jk}\ , \quad j,k=1,2\ . \tag{41}$$

The effect of the kicks on states $|\psi\rangle$ in the Schrödinger picture equivalent to the transformations (40) of the operators is not immediately obvious. A physical interpretation of the action of the kicks on wave functions is given after the introduction of the Floquet operator $U(T)$, which is the subject of the next subsection.

B. The Floquet operator $U(T)$

For any quantum system, the knowledge of the unitary time-evolution operator $U(t,t_0)$ is sufficient in order to propagate an arbitrary state $|\psi\rangle$ from time t_0 up to time t. Yet the evaluation of the formal expression ($\mathfrak{T}$ is the time-ordering operator)

$$U(t,t_0)=\mathfrak{T}\exp\left[-\frac{i}{\hbar}\int_{t_0}^{t}dt\,\hat{H}(t)\right] \tag{42}$$

generally is complicated. However, for the system described by the Hamiltonian Eq. (37) the explicit evaluation of the time-ordered product Eq. (42) is possible due to the particular δ-type time dependence. The Floquet

operator $U(T)$, defined as the time-evolution operator over one period T (see, e.g., [26]), is determined explicitly in Appendix A,

$$U(T)\equiv U(T_{n+1}^-,T_n^-)=U_F(T)U_K \ . \tag{43}$$

The discrete time-translational invariance of the Hamilton operator (37) results in an operator $U(T)$, which is independent of the choice of a particular interval. In addition, it turns out to be a product of two operators. First the kick operator acts

$$U_K=\exp\left[-\frac{i}{2\hbar}(\hat{\mathbf{x}}\cdot\tilde{\mathbf{V}}\cdot\hat{\mathbf{p}}+\hat{\mathbf{p}}\cdot\mathbf{V}\cdot\hat{\mathbf{x}})\right]\equiv\exp\left[-\frac{i}{\hbar}\hat{\mathbf{D}}(\mathbf{V})\right] \tag{44}$$

during an infinitesimally short-time interval including T_n. Here $\hat{\mathbf{D}}(\mathbf{V})$ is a "generalized dilation operator," and the operator U_K represents the integrated form of the operator transformations (38). Subsequently the operator

$$U_F(T)=\exp\left[-\frac{iT}{2\hbar}\hat{\mathbf{p}}^2\right] \tag{45}$$

effects the free-particle propagation during the time interval (T_n^+,T_{n+1}^-). The application of the Floquet operator $U(t)$ to an arbitrary initial state $|\psi\rangle$ can be considered as a "quantum map" [15]. One is interested in the "images" of the initial state $|\psi\rangle$ at times $T,2T,3T,\ldots$ only. The knowledge of the wave function at these discrete times is assumed to be sufficient for the investigation of the long-time behavior—just as a stroboscopical observation of a classical system may reveal chaotic behavior.

The choice of the time interval of periodicity determines the order in which the operators U_K and $U_F(T)$ appear in Eq. (43); another asymmetric version of the Floquet operator is obtained by reversing their order

$$U(T)=U_K U_F(T) \ , \tag{46}$$

whereas the convention

$$U_S(t)=U(T_n+T/2,T_n-T/2)=U_F(T/2)U_K U_F(T/2) \tag{47}$$

would be a symmetric representation of the Floquet operator $U(T)$.

The time evolution of arbitrary states $|\psi\rangle$ is known if the time evolution of the elements of a basis of Hilbert space is known. Two bases prove to be particularly useful. On the one hand, there is the complete set of orthonormal (generalized) eigenvectors of the position operator

$$\hat{\mathbf{x}}|\mathbf{x}\rangle=\mathbf{x}|\mathbf{x}\rangle, \quad x,y\in[0,1) \ , \tag{48}$$

with the property

$$|\mathbf{x}+\mathbf{z}\rangle=|\mathbf{x}\rangle, \quad z_x,z_y\in\mathbb{Z} \ , \tag{49}$$

which follows from tiling the xy plane into equivalent unit squares. On the other hand, there is an orthonormal basis associated with the momentum operator

$$\hat{\mathbf{p}}|\mathbf{p}\rangle=\mathbf{p}|\mathbf{p}\rangle\equiv\hbar\mathbf{k}|\hbar\mathbf{k}\rangle, \quad k_x,k_y\in\mathbb{Z} \ , \tag{50}$$

its discrete spectrum being a consequence of the spatial periodicity.

It is interesting to determine the transformations of position and momentum operators generated by the unitary kick operator U_K. This has been done in Appendix B and one finds

$$\begin{aligned}\hat{\mathbf{x}}'&=U_K^+\hat{\mathbf{x}}U_K=e^{\mathbf{V}\cdot}\hat{\mathbf{x}}\equiv\mathbf{M}\cdot\hat{\mathbf{x}} \ ,\\ \hat{\mathbf{p}}'&=U_K^+\hat{\mathbf{p}}U_K=e^{-\tilde{\mathbf{V}}\cdot}\hat{\mathbf{p}}\equiv\tilde{\mathbf{M}}^{-1}\cdot\hat{\mathbf{p}} \ ,\end{aligned} \tag{51}$$

corresponding exactly to Eqs. (40), which followed from direct integration of the Heisenberg equations.

Further, it is illuminating to determine the action of the kick on the eigenfunctions of position and momentum operators. Consider to this end the eigenvalue equation

$$\hat{\mathbf{x}}|\mathbf{x}\rangle=\mathbf{x}|\mathbf{x}\rangle, \quad x,y\in[0,1) \ . \tag{52}$$

From multiplying this equation with U_K^+ from the left and making use of the first of Eqs. (51) it follows that the state $|\mathbf{x}\rangle'\equiv U_K^+|\mathbf{x}\rangle$ also is an eigenvector of the position operator with eigenvalue $\mathbf{M}^{-1}\cdot\mathbf{x}$

$$\hat{\mathbf{x}}|\mathbf{x}\rangle'=\mathbf{M}^{-1}\cdot\mathbf{x}|\mathbf{x}\rangle' \ . \tag{53}$$

Therefore one necessarily has $|\mathbf{x}\rangle'\equiv|\mathbf{M}^{-1}\cdot\mathbf{x}\rangle$, and from substituting $\mathbf{x}\rightarrow\mathbf{M}\cdot\mathbf{x}$ it follows that

$$U_K|\mathbf{x}\rangle=|\mathbf{M}\cdot\mathbf{x}\rangle \ . \tag{54}$$

The kick U_K operates on the labels of the eigenvectors of $\hat{\mathbf{x}}$ exactly as the map $\mathbf{M}$ acts on the classical configuration space. The elements of the position basis are interchanged according to the hyperbolic map $\mathbf{M}$. The (generalized) orthogonality relations in Hilbert space of the elements of $\{|\mathbf{x}\rangle\}$ and $\{|\mathbf{M}\cdot\mathbf{x}\rangle\}$, respectively, are equivalent. But the relation of "neighborhood" in configuration space changes, a relation which implicitly is contained in the labels $\mathbf{x}$; this observation, as a matter of fact, is the crucial point. States with initially close labels are mapped under the kick transformation to states which do not necessarily have close labels again. As is shown below, this mechanism gives rise to a type of quantum-mechanical motion which mimics chaotic behavior as it is known from classical mechanics.

The transformation of a momentum eigenstate may be derived analogously to the calculation leading to Eq. (54). Here a different way is presented which makes use of the completeness relation

$$\int_\Gamma d\mathbf{x}|\mathbf{x}\rangle\langle\mathbf{x}|=\mathbf{1} \ , \tag{55}$$

where Γ denotes the unit square in the xy plane which is invariant under the map $\mathbf{M}$: $\Gamma'\equiv\mathbf{M}\Gamma=\Gamma$. One easily derives

$$U_K|\mathbf{p}\rangle = U_K \int_\Gamma d\mathbf{x}|\mathbf{x}\rangle\langle\mathbf{x}|\mathbf{p}\rangle = \int_\Gamma d\mathbf{x}|\mathbf{M}\cdot\mathbf{x}\rangle\langle\mathbf{x}|\mathbf{p}\rangle$$
$$= \int_{\Gamma'\equiv\Gamma} d\mathbf{x}|\mathbf{x}\rangle\langle\mathbf{M}^{-1}\cdot\mathbf{x}|\mathbf{p}\rangle = \frac{1}{2\pi\hbar}\int_\Gamma d\mathbf{x}|\mathbf{x}\rangle\exp\left[\frac{i}{\hbar}(\mathbf{x}\cdot\tilde{\mathbf{M}}^{-1})\cdot\mathbf{p}\right]$$
$$= \frac{1}{2\pi\hbar}\int_\Gamma d\mathbf{x}|\mathbf{x}\rangle\exp\left[\frac{i}{\hbar}\mathbf{x}\cdot(\tilde{\mathbf{M}}^{-1}\cdot\mathbf{p})\right]$$
$$= \int_\Gamma d\mathbf{x}|\mathbf{x}\rangle\langle\mathbf{x}|\tilde{\mathbf{M}}^{-1}\cdot\mathbf{p}\rangle = |\tilde{\mathbf{M}}^{-1}\cdot\mathbf{p}\rangle\ . \tag{56}$$

Altogether, the canonical transformation generated by the classical kick has a simple quantum counterpart in the action of U_K on the position and momentum basis. For the following it is of particular importance that the kick U_K does not map an eigenstate of $\hat{\mathbf{x}}$ or $\hat{\mathbf{p}}$ on complicated linear combinations of vectors $|\mathbf{x}\rangle$ or $|\mathbf{p}\rangle$, but that the image of such a state is simply another eigenvector of the *same* operator. This property will make it possible to determine exactly the eigenfunctions and the spectrum of the Floquet operator $U(T)$.

C. Eigenfunctions and spectrum of the Floquet operator

The eigenfunctions $|\psi\rangle$ of the time-evolution operator $U(T)$ can be found by solving the equation

$$U(T)|\psi\rangle = \exp\left[-\frac{iET}{\hbar}\right]|\psi\rangle\ . \tag{57}$$

The set of all numbers E for which Eq. (57) holds is called the quasienergy spectrum, and to each particular value of E there is associated at least one (possibly generalized) eigenstate.

In order to determine the states $|\psi\rangle$ it is helpful to visualize the action of the Floquet operator $U(T)$ in the momentum basis. Imagine the elements of the basis $\{|\mathbf{p}\rangle\}$ to be arranged in a two-dimensional grid, the points of which are labeled by the quantum numbers p_x and p_y. The operator U_K maps any eigenstate $|\mathbf{p}\rangle$ to another eigenstate $|\mathbf{p}\rangle'$ according to Eq. (56). This transformation is unique and invertible. Therefore one can partition the set of all momentum eigenstates $\{|\mathbf{p}\rangle\}$ into disjoint families between which the operator U_K does not induce transitions. For a hyperbolic map $\mathbf{M}$ the families turn out to be a countably infinite number of "discrete hyperbolas" $S(\mathbf{P})$. Each hyperbola can be labeled by an arbitrary point $\mathbf{P}$ belonging to it, e.g., the one nearest to the origin $\mathcal{O}$. The collection of states $S(\mathbf{P})=\{|\tilde{\mathbf{M}}^n\cdot\mathbf{P}\rangle, n\in\mathbb{Z}\}$ constitutes an invariant set of the kick operator U_K, that is,

$$U_K\{|\tilde{\mathbf{M}}^n\cdot\mathbf{P}\rangle\} = \{|\tilde{\mathbf{M}}^n\cdot\mathbf{P}\rangle\}\ . \tag{58}$$

Since the momentum is conserved during the free time evolution, the operator $U_F(T)$ does not induce transitions from one hyperbola $S(\mathbf{P})$ to another. The only effect on vectors $|\mathbf{p}\rangle$ is that they acquire an additional phase from one kick to the next

$$U_F(T)|\mathbf{p}\rangle = \exp\left[-\frac{iT}{2\hbar}\mathbf{p}^2\right]|\mathbf{p}\rangle\ . \tag{59}$$

Therefore the eigenstates of the Floquet operator $U(T)$ have to be superpositions of states belonging to *one* hyperbola $S(\mathbf{P})$ endowed with appropriate phases. As a matter of fact, it can be shown (cf. Appendix C) that the states

$$|\mathbf{P},\alpha\rangle = \frac{1}{\sqrt{2\pi}}\sum_{n=-\infty}^{\infty}\exp\left[-\frac{iT}{2\hbar}\varphi_n(\mathbf{P}) - i\alpha n\right]|\tilde{\mathbf{M}}^n\cdot\mathbf{P}\rangle \tag{60}$$

are indeed eigenfunctions of the operator $U(T)$, that is,

$$U(T)|\mathbf{P},\alpha\rangle = e^{-i\alpha}|\mathbf{P},\alpha\rangle\ . \tag{61}$$

Here α is any real number in the interval $[0,2\pi)$, and the function $\varphi_n(\mathbf{p})$ reads explicitly

$$\varphi_n(\mathbf{p}) = \begin{cases} -\sum_{s=0}^{n-1}\tilde{\mathbf{p}}\cdot\mathbf{M}^s\cdot\tilde{\mathbf{M}}^s\cdot\mathbf{p}, & n\geq 0 \\ \sum_{s=1}^{|n|}\tilde{\mathbf{p}}\cdot\mathbf{M}^{-s}\cdot\tilde{\mathbf{M}}^{-s}\cdot\mathbf{p}, & n\leq 0\ . \end{cases} \tag{62}$$

Hence the quasienergy spectrum

$$E = \frac{\alpha\hbar}{T},\quad \alpha\in[0,2\pi) \tag{63}$$

is absolutely continuous.

Every value E belonging to the spectrum of quasienergies is countably infinite degenerate since there is an analog of the classical constant of motion in Eq. (35). It is straightforward to show that

$$\hat{p}_x'(T_n^-)\hat{p}_y'(T_n^-)U_K = U_K\hat{p}_x'(T_{n+1}^-)\hat{p}_y'(T_{n+1}^-)$$
$$= U_K\hat{p}_x'(T_n^-)\hat{p}_y'(T_n^-)\ , \tag{64}$$

where the second equality is due to the operator equivalent of (34). Hence the quantity $\hat{p}_x'(T_n^-)\hat{p}_y'(T_n^-)$ commutes with the kick operator U_K and with the free time-evolution operator $U_F(T)$. Consequently, one has

$$[\hat{p}_x'\hat{p}_y', U(t',t)] = 0\ . \tag{65}$$

What is the mechanism to make the state $|\mathbf{P},\alpha\rangle$ an

eigenstate of the Floquet operator $U(T)$? In Fig. 1 part of a hyperbola $S(\mathbf{P})$ is depicted, and to every state the associated phase is assigned. First the kick operator U_K shifts the amplitude of the state $|\widetilde{\mathbf{M}}^{-k}\cdot\mathbf{P}\rangle$ to its neighbor $|\widetilde{\mathbf{M}}^{-(k+1)}\cdot\mathbf{P}\rangle$, and subsequently a phase shift occurs generated by the free time evolution $U_F(T)$. Altogether, the effects of the two elements of the time evolution during one period T cancel, except for an overall factor $\exp[-i\alpha]$.

The set of states $\{|\mathbf{P},\alpha\rangle\}$ of Eq. (60) constitutes a (generalized) orthonormal basis of Hilbert space. The completeness relation follows from a straightforward calculation, which is performed in Appendix C, and reads

$$\int_0^{2\pi} d\alpha \sum_{\mathbf{P}} |\mathbf{P},\alpha\rangle\langle\mathbf{P},\alpha| = 1 \ . \tag{66}$$

The sum over $\mathbf{P}$ runs over all different hyperbolas $S(\mathbf{P})$. The orthonormality of two states $|\mathbf{P},\alpha\rangle$ and $|\mathbf{P}',\alpha'\rangle$ turns out to be

$$\langle\mathbf{P},\alpha|\mathbf{P}',\alpha\rangle = \delta(\mathbf{P},\mathbf{P}') \sum_{m=-\infty}^{\infty} \delta(\alpha-\alpha'+2\pi m) \ , \tag{67}$$

where only the term with $m=0$ is relevant, because α is restricted to the interval $[0,2\pi)$. The Kronecker symbol

$$\delta(\mathbf{P},\mathbf{P}') = \begin{cases} 1 & \text{if } \mathbf{P}=\mathbf{P}' \\ 0 & \text{otherwise} \end{cases} \tag{68}$$

expresses the fact that two hyperbolas labeled with different $\mathbf{P}$ and $\mathbf{P}'$ do not have any state in common.

Strictly speaking the states $\{|\mathbf{P},\alpha\rangle\}$ are not elements of the Hilbert space associated with the Hamiltonian $H(\hat{\mathbf{x}},\hat{\mathbf{p}},t)$: the *continuous* label α requires a Dirac-δ-type normalization of the states. A single state $|\mathbf{P},\alpha\rangle$ contains an infinite amount of energy: it is a superposition of an infinite number of momentum eigenstates $|\mathbf{p}\rangle$ with coefficients of modulus one. Nevertheless, the generalized eigenstates of the Floquet operator $U(T)$ can be used in complete analogy to the basis $\{|\mathbf{x}\rangle\}$ of generalized position eigenstates: the construction of physically realizable "wave packets" is possible by superposition of such states.

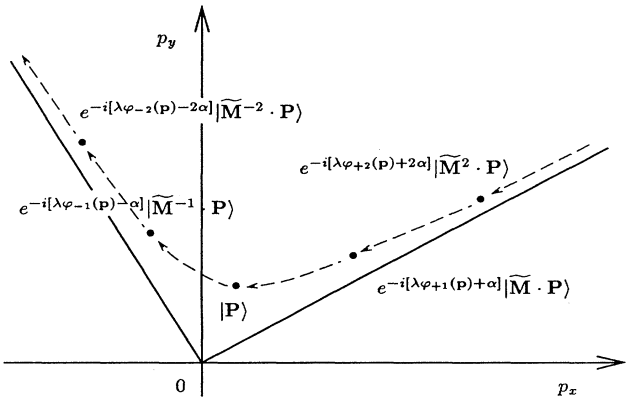

FIG. 1. Some states with correct phases belonging to an eigenstate of the Floquet operator $U(T)$. The action of the kick operator is indicated by arrows and $\lambda = T/2\hbar$.

D. The quantum resonance

The discrete and equidistant spectrum of the momentum operator $\hat{\mathbf{p}}$ has a consequence for which, in a similar context, the term quantum resonance [7] has been coined. If there were no external kicks U_K, any initial state would have built up again exactly after the elapse of a time interval $t_R = 2/h$,

$$|\psi(t_R)\rangle = U_F(t_R)|\psi(0)\rangle = |\psi(0)\rangle \tag{69}$$

since the operator for free time evolution is periodic with t_R,

$$\begin{aligned} U_F(t_R) &= \sum_{\mathbf{p}} U_F(t_R)|\mathbf{p}\rangle\langle\mathbf{p}| = \sum_{\mathbf{p}} \exp\left[-\frac{it_R}{2\hbar}\mathbf{p}^2\right]|\mathbf{p}\rangle\langle\mathbf{p}| \\ &= \sum_{\mathbf{p}} \exp[-2\pi i(k_1^2+k_2^2)]|\mathbf{p}\rangle\langle\mathbf{p}| \\ &= \sum_{\mathbf{p}} |\mathbf{p}\rangle\langle\mathbf{p}| = 1 \ . \end{aligned} \tag{70}$$

In general, the kicking period T of the external fields is completely unrelated to the internal resonance time t_R. If, however, one chooses T to be an integer multiple of the recurrence time t_R,

$$T \equiv T(s) = st_R, \quad s \in \mathbb{N} \ , \tag{71}$$

then the Floquet operator $U(T_n^-(s))$ reduces to a sequence of n kicks

$$U(T_n^-(s)) = (U_F(T(s))U_K)^n = U_K^n \ , \tag{72}$$

and its eigenfunctions simplify to

$$|\mathbf{P},\alpha\rangle = \frac{1}{\sqrt{2\pi}} \sum_{n=-\infty}^{\infty} e^{-i\alpha n}|\widetilde{\mathbf{M}}^n\cdot\mathbf{P}\rangle \ . \tag{73}$$

A study of the quantum-mechanical system may take advantage of the quantum resonances. If the external period T equals the internal recurrence time t_R, then the quantum-mechanical dispersion of wave packets, caused by the free time evolution, is absent in a stroboscopical observation of the system. In other words, it is possible to investigate solely the effect of the "chaos-generating" kicks U_K on the quantum system. Furthermore, the restriction to the resonant situation simplifies the calculation of various time-dependent quantities considerably since the effect of the free time evolution does not have to be taken into account. Free motion of a particle in a two-dimensional region with periodic boundary conditions is well understood; suppressing it for the sake of mathematical convenience by studying the resonant situation will not affect the validity of the general conclusions.

IV. QUANTUM DYNAMICS

A. Irregular behavior of quantum orbits

The irregular behavior of the classical system has its origin in the external perturbation. Without the time-dependent forces all trajectories would evolve regularly in phase space. Associated with the time evolution of a free

particle is the well-known quantum-mechanical dispersion of its wave packet. As was mentioned before, this part of the dynamics is apparently absent in the quantum map if the external period T of the kicks is equal to the internal recurrence time t_R. Thus in order to work out the effect of the linear hyperbolic maps on the quantum-mechanical time evolution the restriction to resonant times $T(s)$ Eq. (71) seems to be promising.

Concentrating for the moment on the time evolution of a generalized position eigenstate $|\mathbf{x}_0\rangle$ one can write down the state reached after an arbitrary number n of periods $T(s)$

$$|\psi(T_n^-(s))\rangle = U_K^n|\mathbf{x}_0\rangle = |\mathbf{M}^n\cdot\mathbf{x}_0\rangle \ , \tag{74}$$

and, consequently, the expectation value of the position operator becomes

$$\langle\psi(T_n^-(s))|\hat{\mathbf{x}}|\psi(T_n^-(s))\rangle = (\mathbf{M}^n\cdot\mathbf{x}_0)\mathrm{mod}1 \ . \tag{75}$$

The time evolution of the expectation value of the position operator $\hat{\mathbf{x}}$ strictly parallels the time evolution of the classical coordinate in the case of vanishing initial momentum or of a classical resonance.

There is an important difference between the classical and the quantum-mechanical model: given a "quantum orbit" consisting of all iterates of some initial state one can calculate all properties of the system at times $T_n^-(s)$. The information about the dynamics as Eq. (74) does not present partial knowledge of the time evolution only, contrary to the classical case. There is no need to think of this "configurational" orbit as a "projection," as it has to be done in the discussion of the classical model.

For the following it is useful to point out a parallel between a classical distribution of initial conditions in a small "configurational volume" (an area) about the point $\mathbf{x}$ with momenta fulfilling the classical resonance condition, Eq. (20), and a superposition of position eigenstates with labels centered about $\mathbf{x}$. The time evolution of both situations in configuration space can be visualized identically.

The mathematical structure of Eqs. (74) and (75) clearly contains elements familiar from the description of classical systems which behave chaotically. The exponential stretching generated by the hyperbolic map $\mathbf{M}$ is accompanied by the mechanism of folding. Does this structure in the quantum system likewise lead to *physical* consequences with an impact on the prediction of the long-time behavior of the system? In other words, does the quantum-mechanical time evolution include physically relevant aspects of "deterministic randomness" as they are familiar from classical mechanics? This question will be answered by investigating the concepts of the Bernoulli shift and of algorithmic complexity in view of Eqs. (74) and (75).

Choose $\mathbf{M}$ for simplicity to be the symmetric cat map C. If only eigenstates of the position operator $\hat{\mathbf{x}}$ are taken into account as initial conditions, the set of all resulting quantum orbits equals the set of all trajectories of the classical Arnold cat map. It is possible to associate the Bernoulli property in two ways with the quantum system.

First, such an association can be worked out in the context of wave functions which, of course, evolve deterministically in time. Yet the sequence of points in the unit square describing the physical state of the system at times $T_n^-(s)$ is governed by a Bernoulli shift with respect to the *labels* of the state. This follows immediately from the equivalence of quantum labels and phase-space points of the classical Arnold cat map. Effectively, the prediction of the long-time behavior becomes extremely difficult on the same grounds as it is familiar from classically chaotic systems.

Second, the association can be established in the context of measurable quantities: the sequence of expectation values $\langle\psi|\hat{\mathbf{x}}(T_n^-(s))|\psi\rangle$ has the Bernoulli property. The difficulty to predict the Hilbert-space state occupied after long times naturally is reflected in the difficulty to predict the expectation value of the position operator and arbitrary functions of it.

In the arguments given above idealized eigenstates of the position operator were considered. The consideration of such physically not realizable idealizations is not necessary: in Sec. IV B the time evolution of states initially localized in a small but finite region of configuration space will be investigated. There is, however, another way to get rid of the idealization related to the continuous spectrum of the position operator. The concept of algorithmic complexity may be applied to the quantum dynamics likewise. It takes into account from the very beginning the inevitably finite numerical accuracy of initial conditions and predictions derived thereof. The arguments given now solely rely on the structure of the Eqs. (74) and (75).

From a numerical point of view there is no difference between the calculation of the classical stroboscopically observed trajectory, Eq. (19), of the time-evolved quantum-mechanical state (74) and the time-dependent expectation value of the position operator $\hat{\mathbf{x}}$ according to Eq. (75). In all three cases the same real numbers have to be calculated, the only difference being their interpretation in physical terms. Henceforth, the algorithmic complexity C_{qm} of the quantum orbits is identical to the complexity C_{cl} of the classical trajectory. In particular, it is different from zero for almost all initial conditions

$$C_{\mathrm{qm}} \equiv C_{\mathrm{cl}} > 0 \ . \tag{76}$$

In the mathematical description of the quantum-mechanical system (37) one thus faces exactly those problems which Ford [27] discussed for classical systems of positive complexity. A principally unavoidable inaccuracy of the initial conditions—including physical and numerical limitations—entails macroscopic irreversibility and the fundamental impossibility of predictions over arbitrarily long times.

The exponential separation of points in configuration space expressing the irregularity of the classical motion can also be observed in the quantum system. However, it is not the Hilbert space metric which is relevant here but the implicit concept of distance contained in the labels of (orthogonal) position eigenstates. A detailed and general investigation of this aspect has been given elsewhere [28]. It has to be emphasized that the "randomness" in the se-

quence of expectation values is a consequence of the probabilistic element of quantum-mechanical predictions, but indeed has its origin in the deterministic time evolution of the wave function. It is easy to devise a gedanken experiment making use of the quantum-mechanical probability in order to produce a truly random number. Imagine a particle of spin $\frac{1}{2}$ prepared in a stationary state with the expectation value of the z component, $\hat{S}_z$, equal to zero

$$|\psi\rangle=\frac{1}{\sqrt{2}}\{|\uparrow\rangle+|\downarrow\rangle\} . \tag{77}$$

Repeated measurements of the operator $\hat{S}_z$ on an ensemble of equivalently prepared systems result in a sequence $\mathcal{S}$ of outcomes $\pm\hbar/2$. This sequence can be considered as binary representation of a real number with the property that 0 and 1 appear equally often. This is enforced by the condition $\langle\psi|\hat{S}_z|\psi\rangle=0$. If there are no hidden variables possessing an integrable dynamics the information contained in $\mathcal{S}$ is algorithmically incompressible or, equivalently, the sequence $\mathcal{S}$ represents an object with positive algorithmic complexity.

B. Expectation values, variances, and correlations

The simple evolution of the momentum operator $\hat{\mathbf{p}}(t)$ over one period T allows one to calculate exactly the long-time behavior of expectation values of momentum and energy with respect to an arbitrary initial state $|\psi(0^-)\rangle$. Estimates of the expectation value of the position operator and its variance are given, which for longer times improve. This is done for a state $|\psi\rangle$ initially localized in configuration space and subject to a resonant sequence of external kicks.

The conservation of momentum during the free motion

$$[U_F(T),\hat{\mathbf{p}}]=0 \tag{78}$$

and the second of Eq. (51) implies the following expression for the Heisenberg operator $\hat{\mathbf{p}}(t)$ directly before the nth kick at time T_n

$$\begin{aligned}\hat{\mathbf{p}}(T_n^-)&=[U^n(T)]^+\hat{\mathbf{p}}(0^-)[U(T)]^n\\&=\tilde{\mathbf{M}}^{-1}\cdot\hat{\mathbf{p}}(T_{n-1}^-)=\cdots=\tilde{\mathbf{M}}^{-n}\cdot\hat{\mathbf{p}}(0^-) .\end{aligned} \tag{79}$$

Assuming for simplicity the matrix $\mathbf{M}$ to be symmetric and using the matrix $\mathbf{D}$ of Eq. (26), which transforms $\mathbf{M}$ to diagonal form $\mathbf{\Lambda}$, one finds

$$\langle\psi|\hat{\mathbf{p}}(T_n^-)|\psi\rangle=\tilde{\mathbf{D}}\cdot\mathbf{\Lambda}^n\cdot\mathbf{D}\cdot\langle\psi|\hat{\mathbf{p}}(0^-)|\psi\rangle . \tag{80}$$

Typically, an arbitrary initial state $|\psi\rangle$ will lead to a nonzero coefficient of the factor $\exp(+n|\ln\lambda|)$ in this expression: the exponential growth of the momenta is generic in this system. The rate of growth is determined by the Lyapunov exponents associated with the classical map $\mathbf{M}$ of the configuration space (or momentum space). As a consequence of the appearance of both $\pm|\ln\lambda|$, there is at the same time an exponential contraction of some component of the initial momentum.

A calculation similar to the one leading to Eq. (80) shows that the expectation value of the energy increases in exact correspondence to the classical quantity. From

$$\begin{aligned}\hat{H}(T_n^-)&=\tfrac{1}{2}\hat{\mathbf{p}}(0^-)\cdot\tilde{\mathbf{M}}^{-2n}\cdot\hat{\mathbf{p}}(0^-)\\&=\tfrac{1}{2}\hat{\mathbf{p}}(0^-)\cdot\tilde{\mathbf{D}}\cdot\mathbf{\Lambda}^{-2n}\cdot\mathbf{D}\cdot\hat{\mathbf{p}}(0^-) ,\end{aligned} \tag{81}$$

where $\mathbf{M}$ again is supposed to be a symmetric matrix, one finds

$$\begin{aligned}\langle\psi|\hat{H}(T_n^-)|\psi\rangle=\tfrac{1}{2}(&e^{n|\ln\lambda^2|}\langle\psi|\hat{p}'^2_{x,0^-}|\psi\rangle\\&+e^{-n|\ln\lambda^2|}\langle\psi|\hat{p}'^2_{y,0^-}|\psi\rangle) ,\end{aligned} \tag{82}$$

showing that for a typical initial state $|\psi\rangle$ the system absorbs energy at an exponential rate for all times.

This fact contrasts with results from an analysis of the standard map and its quantum-mechanical counterpart [7]. Averaged over an ensemble of initial conditions with fixed momentum $\mathbf{p}$ and varying positions, the classical increase of energy turns out to be diffusive, i.e., proportional to time t. Numerical investigations revealed that this behavior has a correspondence in the quantum system for short times t_R only. Later on the so-called "quantum-mechanical suppression of diffusive energy growth" sets in: the expectation value of the energy saturates after the break time t_B. This anomaly in the classical-quantum correspondence was found in such a variety of classically nonintegrable quantum systems that it is considered as one of the manifestations of quantum chaos [29]. Clearly, the results found here do not fit into this scheme.

An important quantity to calculate in time-dependent systems is the momentum auto-correlation function

$$\mathcal{K}^{\mathrm{p}}(\psi,t,t')=\langle\hat{\mathbf{p}}(t):\hat{\mathbf{p}}(t')\rangle_\psi-\langle\hat{\mathbf{p}}(t)\rangle_\psi:\langle\hat{\mathbf{p}}(t')\rangle_\psi , \tag{83}$$

where $(\mathbf{a}:\mathbf{b})_{\alpha\beta}\equiv a_\alpha b_\beta$ denotes the tensor product of two vectors $\mathbf{a}$ and $\mathbf{b}$. The notation $\langle\ \rangle_\psi$ stands for the quantum-mechanical expectation value in the state $|\psi\rangle$. Using $\mathbf{a}:(\mathbf{B}\cdot\mathbf{b})=\mathbf{B}\cdot(\mathbf{a}:\mathbf{b})$ for any matrix $\mathbf{B}$ one can calculate the autocorrelation function with respect to an arbitrary state $|\psi\rangle$

$$\mathcal{K}^p(\psi,t,t')=\tilde{\mathbf{M}}^{-n-n'}\mathcal{K}^{\mathrm{p}}(\psi,0,0) , \tag{84}$$

where n is defined by the condition $T_n^-<t<T_{n+1}^-$ and n' correspondingly. The moduli of the elements of the matrix $\tilde{\mathbf{M}}^n$ grow exponentially with n. Therefore the correlation function $\mathcal{K}^{\mathrm{p}}$ does not approach a limit for $(t'-t)\to\infty$. This behavior is due to the fact that the components of the momenta effectively grow for all times. The momentum autocorrelation of classical particles under the influence of an inverted harmonic-oscillator potential shows the same feature if an average is taken over an ensemble with varying initial momenta.

The trace of the covariance matrix

$$\mathbf{K}^{\mathrm{p}}(\psi,t)=\mathcal{K}^{\mathrm{p}}(\psi,t,t) \tag{85}$$

is equal to the time-dependent variance of the momentum operator which measures the spreading of an arbitrary (initially narrow) momentum distribution. It turns out to be given by

$$\mathrm{tr}\mathbf{K}^p(\psi,T_n^-)=\mathrm{tr}[\tilde{\mathbf{M}}^{-2n}\cdot\mathbf{K}^p(\psi,0^-)] , \tag{86}$$

so that arbitrary initial variances

$$\mathbf{K}^p(\psi,0^-)=\langle(\Delta\hat{p}_x)^2\rangle_\psi+\langle(\Delta\hat{p}_y)^2\rangle_\psi \tag{87}$$

increase unboundedly with an exponential rate $+2|\ln\lambda|$. This is possible because of the classically infinite momentum space.

Expectation values of powers of the position operator $\hat{\mathbf{x}}$ are more difficult to calculate than expectation values of the momentum operator $\hat{\mathbf{p}}$ because there is no analog to Eq. (78). The following results all apply to the special case of a quantum resonance $T\equiv T(s)$ and an initial wave function

$$|\psi\rangle=\frac{1}{\sqrt{\Delta x\,\Delta y}}\int_\Gamma d\mathbf{x}\,\chi(\mathbf{x}_0)|\mathbf{x}\rangle\ . \tag{88}$$

The corresponding probability amplitude $|\psi(\mathbf{x})|^2=\chi(\mathbf{x}_0)/\Delta x\,\Delta y$ is nonzero only in a rectangle centered about $\mathbf{x}_0$

$$\chi(\mathbf{x}_0)=\begin{cases}1, & |x_0-x|\le\Delta x/2,\ |y_0-y|\le\Delta y/2\\ 0 & \text{otherwise}\ ,\end{cases} \tag{89}$$

as shown in Fig. 2. More general distributions $|\psi(\mathbf{x})|^2$ can be approximated arbitrarily well by piecewise constant distributions such as $\chi(\mathbf{x}_0)$.

The expectation value of the operator $\hat{\mathbf{x}}(T_n^-)$ directly before the nth kick is given by

$$\langle\psi|\hat{\mathbf{x}}(T_n^-)|\psi\rangle=\frac{1}{\Delta x\,\Delta y}\int_\Gamma d\mathbf{x}\,\chi(\mathbf{x}_0)(\mathbf{M}^n\cdot\mathbf{x})\text{mod}1\ . \tag{90}$$

Concentrating for the moment on the first component of this equation one has to evaluate the integral

$$I_{RS}(1,\chi(\mathbf{x}_0))=\frac{1}{\Delta x\,\Delta y}\int_\Gamma d\mathbf{x}\,\chi(\mathbf{x}_0)[(Rx+Sy)\text{mod}1]\ ,\qquad R,S\in\mathbb{N}\ , \tag{91}$$

where the elements of the matrix $\mathbf{M}^n$ are

$$\mathbf{M}^n\equiv\begin{bmatrix}R & S\\ T & U\end{bmatrix},\quad R,S,T,U\in\mathbb{Z}\ . \tag{92}$$

Upper and lower bounds of this integral are calculated in Appendix D, leading to the inequality

$$I_{RS}(1,\chi^-(\mathbf{x}_0))\le I_{RS}(1,\chi(\mathbf{x}_0))\le I_{RS}(1,\chi^+(\mathbf{x}_0))\ . \tag{93}$$

Here a grid of $R\times S$ rectangles of size $1/RS$ has been laid on the unit square Γ (see Fig. 3); the characteristic function of the *smallest* rectangle of the RS grid containing the original rectangle is denoted by $\chi^+(\mathbf{x}_0)$, and $\chi^-(\mathbf{x}_0)$, correspondingly, is the characteristic function of the *largest* rectangle of the RS grid contained in the original one. The areas of these rectangles are given by $\Delta R^\pm\Delta S^\pm/RS$, respectively. Inserting the results of Appendix D for the integrals $I_{RS}(1,\chi^\pm(\mathbf{x}_0))$ one finds

$$\frac{1}{2}\frac{\Delta R^-}{R}\frac{\Delta S^-}{S}\le\langle\psi|\hat{x}(T_n^-)|\psi\rangle\le\frac{1}{2}\frac{\Delta R^+}{R}\frac{\Delta S^+}{S}\ . \tag{94}$$

Using the estimates

$$\frac{\Delta R^+}{R}\le\Delta x+\frac{2}{R},\quad \frac{\Delta R^-}{R}\ge\Delta x-\frac{2}{R}\ , \tag{95}$$

and equivalent relations for S one derives

$$\left|\langle\psi|\hat{x}(T_n^-)|\psi\rangle-\frac{1}{2}\right|\le\frac{1}{\Delta xR}+\frac{1}{\Delta yS}+\frac{2}{\Delta x\,\Delta yRS}\ ; \tag{96}$$

an analogous relation holds for the y component of Eq. (90). This result indicates that the expectation value of the position operator $\hat{\mathbf{x}}$ *does* approach a limit (remember that the entries $R,S,\ldots$ of the matrix $\mathbf{M}$ depend on n)

$$\lim_{n\to\infty}\langle\psi|\hat{\mathbf{x}}(T_n^-)|\psi\rangle=\frac{1}{2}\begin{bmatrix}1\\1\end{bmatrix}\ . \tag{97}$$

Thus the continuous quasi-energy spectrum of the Floquet operator $U(T)$ allows for "relaxation" in configuration space. This is in contrast to the well-

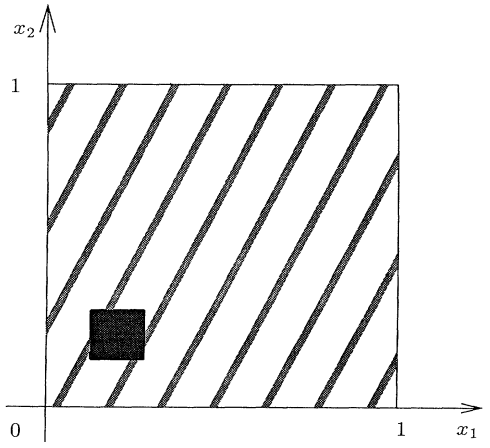

FIG. 2. Distribution of nonzero coefficients of the state $|\psi\rangle$ over the configuration space at time $t=0^-$ (dark square) and after a number of periods (light bands) (schematic representation).

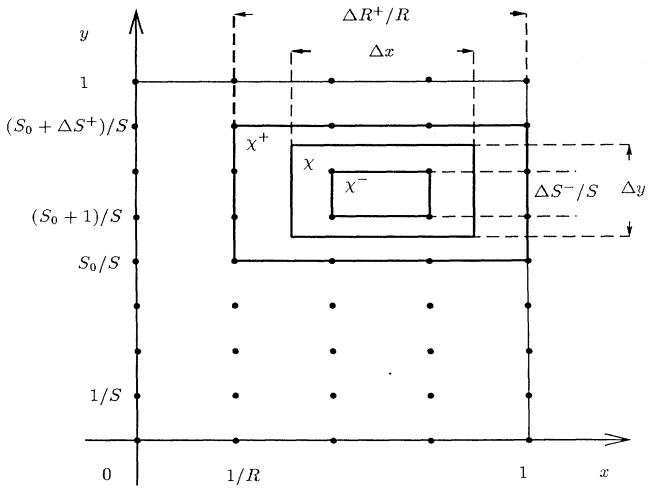

FIG. 3. The grid of RS rectangles used for the calculation of the integrals $I_{RS}(g(\mathbf{x}),\chi(\mathbf{x}_0))$.

known quasiperiodic behavior of expectation values in quantum systems with a discrete energy (or quasienergy) spectrum [30]. Furthermore, the dependence of the matrix elements on n: $R \propto R_0 \exp(n|\ln\lambda|)$, etc. effects an approach to the limit at an *exponential* rate. In other words, the coefficients $(\Delta x \Delta y)^{-1/2}\chi(\mathbf{x}_0)$ of the initial state $|\psi\rangle$ are spread very effectively over the whole set of position eigenstates $|\mathbf{x}\rangle$.

The limiting value, Eq. (97), also is obtained under the assumption that a constant probability distribution over the unit square is given:

$$\int_\Gamma d\mathbf{x}\,\mathbf{x}|\psi(\mathbf{x})|^2 = \int_\Gamma d\mathbf{x}\,\mathbf{x} = \frac{1}{2}\begin{bmatrix}1\\1\end{bmatrix} . \tag{98}$$

However, it is not such a continuous distribution which is approached here: the time evolution in the Schrödinger picture immediately reveals that there is no *continuous* limiting distribution of $|\psi(\mathbf{x}, T_n^-)|^2$ for large n. The unit square is covered by an ever larger number of ever finer parallel bands as it is shown schematically in Fig. 2.

It is interesting to compare this process with the procedure of "coarse graining," which even in mixing systems has to be performed in order to obtain an approach of "macroscopic" observables to equilibrium. In the quantum-mechanical model studied here it is not necessary to introduce a coarse graining by hand: the wave function develops arbitrarily fine structures which are smeared out automatically when going over to expectation values of observables.

The position autocorrelation function contains information about the time evolution of spatial correlations. It is defined in analogy to the momentum autocorrelation function in Eq. (83)

$$\mathcal{K}^{\mathbf{x}}(\psi,t,t') = \langle \hat{\mathbf{x}}(t):\hat{\mathbf{x}}(t')\rangle_\psi - \langle \hat{\mathbf{x}}(t)\rangle_\psi : \langle \hat{\mathbf{x}}(t')\rangle_\psi . \tag{99}$$

One can write

$$\mathcal{K}^{\mathbf{x}}(\psi, T_n^-, T_{n+m}^-) = \mathcal{K}^{\mathbf{x}}(\psi(T_n^-), 0^-, T_m^-) . \tag{100}$$

Suppose the state at time T_n^- to be given by

$$|\tilde{\psi}\rangle = |\psi(T_n^-)\rangle = \frac{1}{\sqrt{\Delta x \Delta y}} \int_\Gamma d\mathbf{x}\,\chi(\mathbf{x}_0)|\mathbf{x}\rangle , \tag{101}$$

with $\chi(\mathbf{x}_0)$ defined as before in Eq. (89). The explicit calculation leads to integrals of the type

$$\mathcal{K}^{\mathbf{x}}_{xx}(\psi(T_n^-),0^-,T_m^-) = \frac{1}{\Delta x \Delta y}\int_\Gamma d\mathbf{x}\,\chi(\mathbf{x}_0) x \times[(Rx+Sy)\bmod 1] \times I_{RS}(x,\chi(\mathbf{x}_0)) . \tag{102}$$

In Appendix D this integral is evaluated approximately leading to the inequality

$$\mathcal{K}^{\mathbf{x}}_{xx}(\psi(T_n^-),0^-,T_m^-) \le \tfrac{1}{2}\langle \hat{\mathbf{x}}(0^-)\rangle_{\tilde{\psi}} + \text{const}\frac{1}{R} + O\left[\frac{1}{R^2}\right] . \tag{103}$$

Thus one has for the correlation function

$$\mathcal{K}^{\mathbf{x}}(\psi(T_n^-),0^-,T_m^-) \le \begin{bmatrix}1/R & 1/S\\ 1/T & 1/U\end{bmatrix} \sim \mathbf{K} e^{-m|\ln\lambda|} , \tag{104}$$

where $\mathbf{K}$ is an m-independent matrix, and terms of $O(1/R^2)$, etc. have been dropped. As a result spatial correlations decay exponentially in time. In classical mechanics such a behavior for correlations of arbitrary phase-space functions is found in K systems showing the property of mixing.

A quantitative measure for the spreading of the state $|\psi\rangle$ over the unit square is given by the trace of covariance matrix

$$\mathbf{K}^{\mathbf{x}}(\psi,t) = \mathcal{K}^{\mathbf{x}}(\psi,t,t) . \tag{105}$$

The integral

$$\langle\psi|\hat{x}^2(T_n^-)|\psi\rangle = \frac{1}{\Delta x \Delta y}\int_\Gamma d\mathbf{x}\,\chi(\mathbf{x}_0)[(Rx+Sy)\bmod 1]^2 = I_{RS}(f_{RS}(\mathbf{x}),\chi(\mathbf{x}_0)) \tag{106}$$

contributes to the upper left element of this matrix. The upper and lower bounds of this quantity (obtained in Appendix D) imply that

$$|\langle\psi|[\Delta\hat{x}(T_n^-)]^2|\psi\rangle - \tfrac{1}{12}| \le c_1 e^{-n|\ln\lambda|} + c_2 e^{-2n|\ln\lambda|} , \tag{107}$$

where

$$\frac{\Delta R^-}{R} \le \Delta x, \quad \frac{\Delta R^+}{R} \ge \Delta x , \tag{108}$$

and equivalent estimates for S have been used. From analogous calculations qualitatively the same behavior follows for the other diagonal element of the covariance matrix. The variances thus relax at an exponential rate to an "equilibrium value" of $\frac{1}{12}$, which is the maximum value possible.

V. CONCLUSIONS

In summary, a physical system with two degrees of freedom has been introduced and investigated analytically in great detail for both a classical and quantum-mechanical description. The most important property of the quantum system is the absolute continuity of the quasienergy spectrum which follows immediately after the construction of the complete set of eigenfunctions of the Floquet operator $U(T)$ has been achieved. In the framework of classical mechanics it is ultimately the continuum of points in phase space which sets the stage for a possible occurrence of chaotic behavior—in quantum mechanics truly chaotic behavior becomes possible due to the continuously labeled set of position basis vectors.

The time evolution of the system shows various features which in classical mechanics are considered as unmistakable characteristics of irregular motion. These features have their origin in the continuous spectrum of quasienergies in combination with the boundedness of the configuration space. The continuity of the spectrum relieves the time dependence of wave functions from being quasiperiodic, and expectation values may tend to an equilibrium value which is approached at an exponential rate; at the same time, spatial autocorrelations decay exponentially. In addition, almost all sequences of time-evolved position eigenstates have been shown to be algo-

rithmically complex. The evolution of continuous spatial distributions inherits these properties in a straightforward manner. It is worthwhile to mention that these results are in complete conformity with Ford and Ilg's result [10] that the time-dependent wave functions of *autonomous bounded* quantum systems are algorithmically compressible.

These features are not commonly observed in typical quantum systems with a classically chaotic counterpart, and, in addition, various tools standard for characterizing such systems do not apply to the present model. Consider, as an example, the random-matrix theory hypothesis [31] establishing a relation between the statistics of *discrete* energy levels of particular quantum systems and those of random matrices belonging to a specific ensemble: a continuous spectrum clearly does not fit into this scheme. Moreover, the model under investigation does not show the widespread anomaly in the correspondence of classical and quantum-mechanical behavior, i.e., the "suppression of diffusive energy growth." On the contrary, the quantum-mechanical expectation value of the energy grows in perfect conformity with the classical quantity.

Another important point should be emphasized: many of the phenomena discussed in the preceding sections are actually linked to the problem of effectively predicting the future behavior of the system. This establishes a further strong parallel to chaotic behavior in classical systems, since many "signatures of quantum chaos" pertain more to "static" properties than to dynamical ones, e.g., the (unfolded) spectrum of energy-level distances, nodal patterns of wave functions, or the occurrence of avoided crossings. The continuous quasienergy spectrum indeed entails consequences which are comparable to problems showing up in the description of classically irregular motion. Any inaccuracy in the determination of the initial quantum state quickly spreads over the total system, rendering it difficult to predict precisely its evolution over long times, albeit the wave functions evolve strictly deterministically. As in classical mechanics this represents a fundamental limitation of the statements one can make about the system. A general theory concerning the actual observation of this kind of irregular behavior and its actual observation by means of quantum nondemolition measurements has been given elsewhere [28].

For further discussions of "sensitive dependence" and similar concepts in quantum mechanics the reader is referred to work by, e.g., Jensen [32], Luna-Acosta [33], and Mendes [34]. Recently, Mendes [35] provided a general approach to this problem in which the importance of "δ'-type interactions" (i.e., the momentum dependence of the kick amplitude in the present model) for the occurrence of nonvanishing quantum Lyapunov exponents is pointed out.

Much work has been devoted to the question under what circumstances ergodic behavior or mixing in driven systems may occur. Discrete quasienergy spectra in combination with bounded systems lead to wave functions which are quasiperiodic in time, and hence the decay of correlation functions is excluded. There are two prominent types of systems without strict time periodicity which are known to exhibit ergodic behavior. Shepelyansky [11] introduced a kicked rotator subject to a quasiperiodic driving force; the suppression of diffusive energy growth turned out to be no longer as pronounced as it is in the periodically kicked system. Geisel [30] investigated a quasiperiodically kicked spin-$\frac{1}{2}$ model, but on long time scales no evidence for statistical properties such as the decay of correlations was observed. Later, Shepelyansky [11] and Toda, Adachi, and Ikeda [36] considered a model in which originally periodic kick times are replaced by a stochastic sequence: numerical experiments indeed show that macroscopic reversibility is no longer present. This result is considered to be equivalent to the existence of mixing behavior in the quantum time evolution. Introducing external noise, however, does not bear on the question whether deterministic randomness is present in quantum dynamics.

The results obtained for the present model indicate that macroscopic irreversibility, one of the hallmarks of chaotic behavior, is at least principally realizable in time-periodic quantum systems. Consider the situation investigated in Sec. IV. Suppose a state $|\psi\rangle$, which in configuration space is a narrow wave packet, is propagated from time t_i up to t_f. The backward iteration, after having transformed $|\psi\rangle$ into $|\psi\rangle^*$ (if magnetic fields $\mathbf{B}$ are involved they have to be transformed into $-\mathbf{B}$) certainly does not lead to the original state $|\psi\rangle$ or the associated probability distribution. This effect is due to the exponential separation of the coefficients of position eigenstates which has been discussed in detail.

In conclusion, the time evolution of the model introduced here allows one to pinpoint one possible origin of irregularity in the quantum-mechanical motion. The local instability, generated by a hyperbolic map acting in configuration space, transforms the continuous labels of position eigenstates just as the coordinates of the corresponding classical system and, henceforth, it renders the time evolution deterministically random.

ACKNOWLEDGMENTS

I would like to thank the Schweizer Nationalfonds and the Freiwillige Akademische Gesellschaft (Basel) for partial financial support of this work.

APPENDIX A: THE FLOQUET OPERATOR

In this appendix the explicit form of the time-evolution operator $U(t',t)$ over one period, the Floquet operator $U(T)\equiv U(T^-,0^-)$, is determined.

First of all, one may break the time evolution into two parts

$$U(T^-,0^-)=U(T^-,0^+)U(0^+,0^-)\,, \tag{A1}$$

where, for notational convenience, the kick operator acts first. For definiteness it is appropriate to perform the calculations with finite ϵ and to take the limit $\epsilon\to 0$ at the end. One can write

$$U^{(\epsilon)}(T)=U(T-\epsilon,-\epsilon)=U(T-\epsilon,+\epsilon)U(+\epsilon,-\epsilon)$$
$$=U_F^{(\epsilon)}(T)U_K^{(\epsilon)}\ , \tag{A2}$$

with $\epsilon \ll 1$ being a finite positive number. The first term representing the free time evolution from $+\epsilon$ to $T-\epsilon$ immediately gives

$$U_F^{(\epsilon)}(T)=U(T-\epsilon,+\epsilon)=\exp\left[-\frac{i(T-2\epsilon)}{2\hbar}\hat{\mathbf{p}}^2\right]\ . \tag{A3}$$

The second part follows from evaluating

$$U_K^{(\epsilon)}=\mathfrak{T}\exp\left[-\frac{i}{\hbar}\int_{-\epsilon}^{+\epsilon}dt\,\hat{H}_\epsilon(t)\right]$$
$$=\sum_{n=0}^{\infty}\frac{1}{n!}\mathfrak{T}\left[\frac{i}{\hbar}\int_{-\epsilon}^{+\epsilon}dt\,\hat{H}_\epsilon(t)\right]^n\ , \tag{A4}$$

where

$$\hat{H}_\epsilon(t)=\tfrac{1}{2}\hat{\mathbf{p}}^2+V(\hat{\mathbf{x}},\hat{\mathbf{p}})\Delta_{T,\epsilon}(t)=\mathcal{T}+V\Delta_{T,\epsilon}(t)\ , \tag{A5}$$

with the abbreviations $\mathcal{T}$ and V for the operators of kinetic and potential energy, respectively. The kick operator reads

$$U_K^{(\epsilon)}=1+\left[-\frac{i}{\hbar}\right]\int_{-\epsilon}^{+\epsilon}dt\,\hat{H}_\epsilon(t)+\left[-\frac{i}{\hbar}\right]^2\int_{-\epsilon}^{+\epsilon}dt_1\int_{-\epsilon}^{t_1}dt_2\hat{H}_\epsilon(t_1)\hat{H}_\epsilon(t_2)$$
$$+\left[-\frac{i}{\hbar}\right]^3\int_{-\epsilon}^{+\epsilon}dt\int_{-\epsilon}^{t}dt_1\int_{-\epsilon}^{t_1}dt_2\hat{H}_\epsilon(t)\hat{H}_\epsilon(t_1)\hat{H}_\epsilon(t_2)+\cdots$$
$$=1+\left[-\frac{i}{\hbar}\right]\{\mathcal{T}(2\epsilon)+V\}+\left[-\frac{i}{\hbar}\right]^2\int_{-\epsilon}^{+\epsilon}dt_1\int_{-\epsilon}^{t_1}dt_2\{\mathcal{T}^2+\mathcal{T}V\Delta_\epsilon(2)+V\mathcal{T}\Delta_\epsilon(1)+V^2\Delta_\epsilon(1)\Delta_\epsilon(2)\}$$
$$+\left[-\frac{i}{\hbar}\right]^3\int_{-\epsilon}^{+\epsilon}dt_1\int_{-\epsilon}^{t_1}dt_2\int_{-\epsilon}^{t_2}dt_3\{\mathcal{T}^3+\mathcal{T}^2V\Delta_\epsilon(3)+\mathcal{T}V\mathcal{T}\Delta_\epsilon(2)+V\mathcal{T}^2\Delta_\epsilon(1)+\mathcal{T}V^2\Delta_\epsilon(2)\Delta_\epsilon(3)$$
$$+V\mathcal{T}V\Delta_\epsilon(1)\Delta_\epsilon(3)+V^2\mathcal{T}\Delta_\epsilon(1)\Delta_\epsilon(2)+V^3\Delta_\epsilon(1)\Delta_\epsilon(2)\Delta_\epsilon(3)\}+\ldots, \tag{A6}$$

where $\Delta_\epsilon(1)$ is a shorthand for $\delta_\epsilon(t_1)$, etc. Performing the integrals and rearranging the terms yield

$$U_K^{(\epsilon)}=1+\left[-\frac{i}{\hbar}\right]\{\mathcal{T}(2\epsilon)+V\}+\left[-\frac{i}{\hbar}\right]^2\left\{\mathcal{T}^2\frac{1}{2}(2\epsilon)^2+(\mathcal{T}V+V\mathcal{T})\epsilon+\frac{1}{2}V^2\right\}$$
$$+\left[-\frac{i}{\hbar}\right]^3\{\mathcal{T}^3O(\epsilon^3)+(\mathcal{T}^2V+\cdots)O(\epsilon^2)+(\mathcal{T}V^2+\cdots)O(\epsilon)+\frac{1}{3!}V^3\}+\cdots \tag{A7}$$
$$=1+\left[-\frac{i}{\hbar}\right]V+\frac{1}{2!}\left[-\frac{i}{\hbar}\right]^2V^2+\frac{1}{3!}\left[-\frac{i}{\hbar}\right]^3V^3+\cdots+O(\epsilon)=\exp\left[-\frac{i}{\hbar}V\right][1+O(\epsilon)+\cdots]\ .$$

Consequently, the Floquet operator $U(T)$ becomes

$$U(T)=\lim_{\epsilon\to 0}U^{(\epsilon)}(T)=\lim_{\epsilon\to 0}U_K^{(\epsilon)}U_F^{(\epsilon)}(T)$$
$$=\exp\left[-\frac{iT}{2\hbar}\hat{\mathbf{p}}^2\right]\exp\left[-\frac{i}{\hbar}V(\hat{\mathbf{x}},\hat{\mathbf{p}})\right]=U_F(T)U_K\ . \tag{A8}$$

APPENDIX B: THE KICK TRANSFORMATION

It is shown that the momentum $\hat{\mathbf{p}}$ and the position operators $\hat{\mathbf{x}}$ transform under the kick U_K according to

$$U_K^+\hat{\mathbf{x}}U_K=e^{\mathbf{V}\cdot}\hat{\mathbf{x}},\quad U_K^+\hat{\mathbf{p}}U_K=e^{-\tilde{\mathbf{V}}\cdot}\hat{\mathbf{p}}\ . \tag{B1}$$

From

$$U_K=\exp\left[-\frac{i}{2\hbar}(\hat{\mathbf{x}}\cdot\tilde{\mathbf{V}}\cdot\hat{\mathbf{p}}+\hat{\mathbf{p}}\cdot\mathbf{V}\cdot\hat{\mathbf{x}})\right]\equiv e^{-\hat{\mathcal{D}}} \tag{B2}$$

it follows that [37]

$$\hat{\mathbf{x}}'=e^{\hat{\mathcal{D}}}\hat{\mathbf{x}}e^{-\hat{\mathcal{D}}}=\sum_{n=0}^{\infty}\frac{1}{n!}[\hat{\mathcal{D}},\hat{\mathbf{x}}]_{(n)}\ , \tag{B3}$$

where

$$[\hat{\mathcal{D}},\hat{\mathbf{x}}]_{(n+1)}=[\hat{\mathcal{D}},[\hat{\mathcal{D}},\hat{\mathbf{x}}]_{(n)}]\ , \tag{B4}$$

with $n\in\mathbb{N}$. One finds successively

$$[\hat{\mathcal{D}},\hat{\mathbf{x}}]_{(1)}=\frac{i}{2\hbar}[\hat{\mathbf{x}}\cdot\tilde{\mathbf{V}}\cdot\hat{\mathbf{p}}+\mathbf{V}\cdot\hat{\mathbf{x}},\hat{\mathbf{x}}]=\mathbf{V}\cdot\hat{\mathbf{x}}\ ,$$
$$[\hat{\mathcal{D}},\hat{\mathbf{x}}]_{(n)}=\mathbf{V}^n\cdot\hat{\mathbf{x}},\quad n\in\mathbb{N}\ , \tag{B5}$$

so that

$$\hat{\mathbf{x}}'=\sum_{n=0}^{\infty}\frac{1}{n!}\mathbf{V}^n\cdot\hat{\mathbf{x}}=e^{\mathbf{V}}\cdot\hat{\mathbf{x}}\ , \tag{B6}$$

and, along the same lines

$$\hat{\mathbf{p}}'=\sum_{n=0}^{\infty}\frac{1}{n!}(-\tilde{\mathbf{V}})^n\cdot\hat{\mathbf{p}}=e^{-\tilde{\mathbf{V}}}\cdot\hat{\mathbf{p}}\ , \tag{B7}$$

what was to be shown.

APPENDIX C: THE STATES $|\mathbf{P},\alpha\rangle$

In this appendix it is shown that the states $|\mathbf{P},\alpha\rangle$ are eigenfunctions of the Floquet operator $U(T)$ and constitute a complete orthonormal set.

First of all, it will be shown that the states

$$|\mathbf{P},\alpha\rangle=\frac{1}{\sqrt{2\pi}}\sum_{n=-\infty}^{\infty}\exp\left[-\frac{iT}{2\hbar}\varphi_n(\mathbf{P})-i\alpha n\right]|\tilde{\mathbf{M}}^n\cdot\mathbf{P}\rangle \tag{C1}$$

are eigenfunctions of the Floquet operator $U(T)$,

$$U(T)|\mathbf{P},\alpha\rangle\equiv U_F(T)U_K|\mathbf{P},\alpha\rangle=e^{-i\alpha}|\mathbf{P},\alpha\rangle\ , \tag{C2}$$

where α is any real number in the interval $[0,2\pi)$ and the function $\varphi_n(\mathbf{p})$ is defined as

$$\varphi_n(\mathbf{p})=\begin{cases}-\sum_{s=0}^{n-1}\tilde{\mathbf{p}}\cdot\mathbf{M}^s\cdot\tilde{\mathbf{M}}^s\cdot\mathbf{p}, & n\geq 0\\ \sum_{s=1}^{|n|}\tilde{\mathbf{p}}\cdot\mathbf{M}^{-s}\cdot\tilde{\mathbf{M}}^{-s}\cdot\mathbf{p}, & n\leq 0\ .\end{cases} \tag{C3}$$

This can be seen as follows. With the use of Eq. (56) the action of the kick U_K on the state $|\mathbf{P},\alpha\rangle$ yields

$$U_K|\mathbf{P},\alpha\rangle=\frac{1}{\sqrt{2\pi}}\sum_{n=-\infty}^{\infty}\exp\left[-\frac{iT}{2\hbar}\varphi_n(\mathbf{P})-i\alpha n\right]\times|\tilde{\mathbf{M}}^{n-1}\cdot\mathbf{P}\rangle\ . \tag{C4}$$

Renaming the index $n\rightarrow n+1$ and applying the operator $U_F(T)$ leads to

$$U_F(T)U_K|\mathbf{P},\alpha\rangle=e^{-i\alpha}\frac{1}{\sqrt{2\pi}}\sum_{n=-\infty}^{\infty}\exp\left[-\frac{iT}{2\hbar}\varphi_{n+1}(\mathbf{P})-i\alpha n\right]\exp\left[-\frac{iT}{2\hbar}\tilde{\mathbf{p}}\cdot\mathbf{M}^n\cdot\tilde{\mathbf{M}}^n\cdot\mathbf{P}\right]|\tilde{\mathbf{M}}^n\cdot\mathbf{P}\rangle$$
$$=e^{-i\alpha}|\mathbf{P},\alpha\rangle\ , \tag{C5}$$

where the last equality only holds if

$$\varphi_{n+1}(\mathbf{p})+\tilde{\mathbf{p}}\cdot\mathbf{M}^n\cdot\tilde{\mathbf{M}}^n\cdot\mathbf{p}=\varphi_n(\mathbf{p}) \tag{C6}$$

is true for all $n\in\mathbb{Z}$. It is necessary to consider four separate cases: (i) $n>0$, (ii) $n=0$, (iii) $n=-1$, and (iv) $n<-1$.

(i) $n>0$: Writing down $\varphi_{n+1}(\mathbf{p})$ explicitly gives

$$\varphi_{n+1}(\mathbf{p})=-\sum_{s=0}^{n}\tilde{\mathbf{p}}\cdot\mathbf{M}^s\cdot\tilde{\mathbf{M}}^s\cdot\mathbf{p}$$
$$=-\sum_{s=0}^{n-1}\tilde{\mathbf{p}}\cdot\mathbf{M}^s\cdot\tilde{\mathbf{M}}^s\cdot\mathbf{p}-\tilde{\mathbf{p}}\cdot\mathbf{M}^n\cdot\tilde{\mathbf{M}}^n\cdot\mathbf{p}$$
$$=\varphi_n(\mathbf{p})-\tilde{\mathbf{p}}\cdot\mathbf{M}^n\cdot\tilde{\mathbf{M}}^n\cdot\mathbf{p}\ , \tag{C7}$$

so that Eq. (C6) holds.

(ii) $n=0$: Because of

$$\varphi_1(\mathbf{p})=-\tilde{\mathbf{p}}\cdot\mathbf{p},\quad \varphi_0(\mathbf{p})=0\ , \tag{C8}$$

Eq. (C6) is fulfilled again.

(iii) $n=-1$: Using

$$\varphi_{-1}(\mathbf{p})=\sum_{s=1}^{|-1|}\tilde{\mathbf{p}}\cdot\mathbf{M}^{-s}\cdot\tilde{\mathbf{M}}^{-s}\cdot\mathbf{p}=\tilde{\mathbf{p}}\cdot\mathbf{M}^{-1}\cdot\tilde{\mathbf{M}}^{-1}\cdot\mathbf{p} \tag{C9}$$

together with Eq. (C8) one gets

$$\varphi_0(\mathbf{p})+\tilde{\mathbf{p}}\cdot\mathbf{M}^{-1}\cdot\tilde{\mathbf{M}}^{-1}\cdot\mathbf{p}=\varphi_{-1}(\mathbf{p})\ . \tag{C10}$$

(iv) $n<-1$: Because of $|n+1|=|n|-1$ one finds

$$\varphi_{n+1}(\mathbf{p})=\sum_{s=1}^{|n|-1}\tilde{\mathbf{p}}\cdot\mathbf{M}^{-s}\cdot\tilde{\mathbf{M}}^{-s}\cdot\mathbf{p}$$
$$=\varphi_n(\mathbf{p})-\tilde{\mathbf{p}}\cdot\mathbf{M}^n\cdot\tilde{\mathbf{M}}^n\cdot\mathbf{p}\ , \tag{C11}$$

which completes the proof of Eq. (C6). Consequently, the states $|\mathbf{P},\alpha\rangle$ are eigenstates of the Floquet operator $U(T)$ with the eigenvalue $\exp[-i\alpha]$.

A straightforward calculation shows that the set of states $|\mathbf{P},\alpha\rangle$ is complete,

$$\int_0^{2\pi}d\alpha\sum_{\mathbf{P}}|\mathbf{P},\alpha\rangle\langle\mathbf{P},\alpha|=\frac{1}{2\pi}\int_0^{2\pi}d\alpha\sum_{\mathbf{P}}\sum_{n,m}\exp\left[-\frac{iT}{2\hbar}[\varphi_n(\mathbf{P})-\varphi_m(\mathbf{P})]\right]\exp[-i\alpha(m-n)]|\tilde{\mathbf{M}}^n\cdot\mathbf{P}\rangle\langle\tilde{\mathbf{M}}^m\cdot\mathbf{P}|$$
$$=\sum_{\mathbf{P}}\sum_{n,m}\exp\left[-\frac{iT}{2\hbar}[\varphi_n(\mathbf{P})-\varphi_m(\mathbf{P})]\right]\delta_{n,m}|\tilde{\mathbf{M}}^n\cdot\mathbf{P}\rangle\langle\tilde{\mathbf{M}}^m\cdot\mathbf{P}|$$
$$=\sum_{\mathbf{P}}\sum_{n}|\tilde{\mathbf{M}}^n\cdot\mathbf{P}\rangle\langle\tilde{\mathbf{M}}^n\cdot\mathbf{P}|\equiv\sum_{\mathbf{p}}|\mathbf{p}\rangle\langle\mathbf{p}|=1\ , \tag{C12}$$

where the sum over $\mathbf{P}$ runs over all different hyperbolas $S(\mathbf{P})$.

Finally, the orthonormality of two states $|\mathbf{P},\alpha\rangle$ and $|\mathbf{P}',\alpha'\rangle$ is seen to follow from the relation

$$\langle \mathbf{P},\alpha|\mathbf{P}',\alpha'\rangle=\frac{1}{2\pi}\sum_{n,m}\exp\left[-\frac{iT}{2\hbar}[\varphi_m(\mathbf{P})-\varphi_n(\mathbf{P})]\right]\exp[-i(\alpha' m-\alpha n)]\langle \tilde{\mathbf{M}}^n\cdot\mathbf{P}|\tilde{\mathbf{M}}^m\cdot\mathbf{P}'\rangle$$

$$=\frac{1}{2\pi}\delta(\mathbf{P},\mathbf{P}')\sum_{m=-\infty}^{\infty}e^{i(\alpha-\alpha')m}=\delta(\mathbf{P},\mathbf{P}')\sum_{m=-\infty}^{\infty}\delta(\alpha-\alpha'+2\pi m)\ , \tag{C13}$$

where only the $m=0$ term is relevant, α being restricted to $[0,2\pi)$. The Kronecker symbol

$$\delta(\mathbf{P},\mathbf{P}')=\begin{cases}1 & \text{if } \mathbf{P}=\mathbf{P}'\\ 0 & \text{otherwise}\end{cases} \tag{C14}$$

stems from the fact that two hyperbolas labeled by $\mathbf{P}$ and $\mathbf{P}'$ never have any state in common.

From a technical point of view it is interesting to note that in the position representation the eigenvalue equation (C5) turns out to be a functional-integral equation

$$\psi(\mathbf{M}^{-1}\cdot\mathbf{x})=\frac{e^{-i\alpha}}{(2\pi\hbar)^2}\int_\Gamma d\mathbf{x}'\theta_3(e^{iT/2\hbar},\mathbf{x}-\mathbf{x}')\psi(\mathbf{x}')\ , \tag{C15}$$

the kernel being a two-dimensional Jacobian theta function

$$\theta_3(e^{i\beta},\mathbf{z})=\sum_{\mathbf{p}}\exp\left[\frac{i}{\hbar}\mathbf{p}\cdot\mathbf{z}+i\beta\mathbf{p}^2\right]\ . \tag{C16}$$

APPENDIX D: THE INTEGRALS $I_{RS}(g(\mathbf{x}),\chi(\mathbf{x}_0))$

In this appendix estimates of the integral

$$I_{RS}(g(\mathbf{x}),\chi(\mathbf{x}_0))$$

$$=\frac{1}{\Delta x\,\Delta y}\int_\Gamma d\mathbf{x}\,\chi(\mathbf{x}_0)g(\mathbf{x})[(Rx+Sy)\text{mod}1]\ ,$$

$$R,S\in\mathbb{N} \tag{D1}$$

are given for various (piecewise) continuous positive functions $g(\mathbf{x})$. Γ denotes the unit square in the xy plane and $\chi(\mathbf{x}_0)$ is the characteristic function of a rectangle of area $\Delta x\,\Delta y$ about the point $\mathbf{x}_0\in\Gamma$

$$\chi(\mathbf{x}_0)=\begin{cases}1, & |x_0-x|\le\Delta x/2,\ |y_0-y|\le\Delta y/2\\ 0 & \text{otherwise}\ .\end{cases} \tag{D2}$$

The function $f_{RS}(\mathbf{x})=(Rx+Sy)\text{mod}1$ is easily visualized. Imagine the plane $(Rx+Sy)=0$ defined over the unit square. The (mod1)-prescription turns it into a "two-dimensional sawtooth," such that the resulting $(R+S)$ disconnected strips are parallel to the original plane.

In order to proceed with the evaluation of the integral in Eq. (D1) it is convenient to decompose the unit square into RS rectangles of size $1/RS$, each of which is divided into two triangles (see Fig. 4)

$$G_{rs}^{(1)}=\left\{x,y\ \middle|\ \frac{r}{R}\le x<\frac{r+1}{R};\frac{s}{S}\le y<\frac{r+s+1-Rx}{S}\right\} \tag{D3}$$

and

$$G_{rs}^{(2)}=\left\{x,y\ \middle|\ \frac{r}{R}\le x<\frac{r+1}{R};\frac{r+s+1-Rx}{S}\le y<\frac{s+1}{S}\right\}\ , \tag{D4}$$

where $r=0,1,\ldots,R-1$ and $s=0,1,\ldots,S-1$. In these regions the function $f_{RS}(\mathbf{x})$ equals

$$f_{rs}^{(1)}(\mathbf{x})=Rx+Sy-(r+s)\ , \tag{D5}$$

$$f_{rs}^{(2)}(\mathbf{x})=Rx+Sy-(r+s+1)\ , \tag{D6}$$

respectively.

In general, the borders of the region characterized by $\chi(\mathbf{x}_0)$ do not fit with the rectangular grid defined by the integers R and S. Let $\chi^+(\mathbf{x}_0)$ be the *smallest* rectangle of the grid *containing* $\chi(\mathbf{x}_0)$, and let $\chi^-(\mathbf{x}_0)$ be the *largest* rectangle of the grid which *is contained* in $\chi(\mathbf{x})$. The cor-

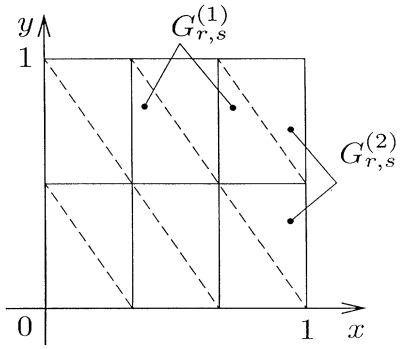

FIG. 4. Definition of the triangular regions $G_{rs}^{(1)}$ and $G_{rs}^{(2)}$, respectively.

responding areas fulfill the inequality

$$\frac{\Delta R^-}{R}\frac{\Delta S^-}{S} \le \Delta x\,\Delta y \le \frac{\Delta R^+}{R}\frac{\Delta S^+}{S} \tag{D7}$$

leading to the relation

$$I_{RS}(g(\mathbf{x}),\chi^-(\mathbf{x}_0)) \le I_{RS}(g(\mathbf{x}),\chi(\mathbf{x}_0)) \le I_{RS}(g(\mathbf{x}),\chi^+(\mathbf{x}_0)) \; . \tag{D8}$$

The integrals $I_{RS}(g(\mathbf{x}),\chi^{\pm}(\mathbf{x}_0))$ can be written as

$$I_{RS}(g(\mathbf{x}),\chi^{\pm}(\mathbf{x}_0)) = \frac{1}{\Delta x\,\Delta y}\sum_{r=R_0^{\pm}}^{R_0+\Delta R^{\pm}}\sum_{r=S_0^{\pm}}^{S_0+\Delta S^{\pm}}\left\{\int_{G_{rs}^{(1)}} d\mathbf{x}\, g(\mathbf{x}) f_{rs}^{(1)}(\mathbf{x}) + \int_{G_{rs}^{(2)}} d\mathbf{x}\, g(\mathbf{x}) f_{rs}^{(2)}(\mathbf{x})\right\} . \tag{D9}$$

The meaning of the numbers R_0 and $\Delta R^{\pm}$ can be inferred from Fig. 3. For ever larger values of R and S the rectangular grid in the unit square gets ever finer and the integrals $I_{RS}(g(\mathbf{x}),\chi^{\pm}(\mathbf{x}_0))$ approach the original one, $I_{RS}(g(\mathbf{x}),\chi(\mathbf{x}_0))$, from above and below.

The upper and lower bounds of $I_{RS}(g(\mathbf{x}),\chi^{\pm}(\mathbf{x}_0))$ are calculated for the functions (i) $g(\mathbf{x})=1$, (ii) $g(\mathbf{x})=x$, and (iii) $g(\mathbf{x})=f_{RS}(\mathbf{x})$.

(i) In this case one finds

$$\begin{aligned} I_{RS}(1,\chi^{\pm}(\mathbf{x}_0)) &= \frac{1}{\Delta x\,\Delta y}\sum_{r=R_0^{\pm}}^{R_0+\Delta R^{\pm}}\sum_{r=S_0^{\pm}}^{S_0+\Delta S^{\pm}}\left\{\int_{r/R}^{(r+1)/R} dx \int_{s/S}^{(r+s+1-Rx)/S} dy\,[Rx+Sy-(r+s)]\right. \\ &\qquad \left. + \int_{r/R}^{(r+1)/R} dx \int_{(r+s+1-Rx)/S}^{(s+1)/S} dy\,[Rx+Sy-(r+s+1)]\right\} \\ &= \frac{1}{\Delta x\,\Delta y}\sum_{r=R_0^{\pm}}^{R_0+\Delta R^{\pm}}\sum_{r=S_0^{\pm}}^{S_0+\Delta S^{\pm}}\left\{\frac{1}{3RS}+\frac{1}{6RS}\right\} = \frac{1}{2}\frac{\Delta R^{\pm}/R}{\Delta x}\frac{\Delta S^{\pm}/S}{\Delta y} \; . \end{aligned} \tag{D10}$$

(ii) A similar calculation yields

$$\begin{aligned} I_{RS}(x,\chi^{\pm}(x_0)) &= \frac{1}{\Delta x\,\Delta y}\sum_{r=R_0^{\pm}}^{R_0+\Delta R^{\pm}}\sum_{r=S_0^{\pm}}^{S_0+\Delta S^{\pm}}\left\{\int_{r/R}^{(r+1)/R} dx \int_{s/S}^{(r+s+1-Rx)/S} dy\, x\,[Rx+Sy-(r+s)]\right. \\ &\qquad \left. + \int_{r/R}^{(r+1)/R} dx \int_{(r+s+1-Rx)/S}^{(s+1)/S} dy\, x\,[Rx+Sy-(r+s+1)]\right\} \\ &= \frac{1}{\Delta x\,\Delta y}\sum_{r=R_0^{\pm}}^{R_0+\Delta R^{\pm}}\sum_{r=S_0^{\pm}}^{S_0+\Delta S^{\pm}}\left\{\frac{8r+3}{24R^2S}+\frac{4r+3}{24R^2S}\right\} \\ &= \frac{\Delta R^{\pm}/R}{\Delta x}\frac{\Delta S^{\pm}/S}{\Delta y}\left\{\frac{1}{2}\left[\frac{R_0^{\pm}}{R}+\left[\frac{\Delta R_0^{\pm}/R}{\Delta x}\right]\frac{\Delta x}{2}\right]+\frac{1}{2R}\left[\frac{R_0^{\pm}}{R}+\frac{1}{2}\right]\right\} , \end{aligned} \tag{D11}$$

where the first term in the curly brackets is of $O(1)$ approaching $\langle \hat{x} \rangle_{\psi}$ and the second one is of order $O(1/R)$.

(iii) In this case one obtains

$$\begin{aligned} I_{RS}(f_{RS}(\mathbf{x}),\chi^{\pm}(\mathbf{x}_0)) &= \frac{1}{\Delta x\,\Delta y}\sum_{r=R_0^{\pm}}^{R_0+\Delta R^{\pm}}\sum_{r=S_0^{\pm}}^{S_0+\Delta S^{\pm}}\left\{\int_{r/R}^{(r+1)/R} dx \int_{s/S}^{(r+2+1-Rx)/S} dy\,[Rx+Sy-(r+s)]^2\right. \\ &\qquad \left. + \int_{r/R}^{(r+1)/R} dx \int_{(r+s+1-Rx)/S}^{(s+1)/S} dy\,[Rx+Sy-(r+s+1)]^2\right\} \\ &= \frac{1}{\Delta x\,\Delta y}\sum_{r=R_0^{\pm}}^{R_0+\Delta R^{\pm}}\sum_{r=S_0^{\pm}}^{S_0+\Delta S^{\pm}}\left\{\frac{1}{4RS}+\frac{1}{12RS}\right\} = \frac{1}{3}\frac{\Delta R^{\pm}/R}{\Delta x}\frac{\Delta S^{\pm}/S}{\Delta y} \; . \end{aligned} \tag{D12}$$

MACSYMA [38] has been used for these calculations.

[1] *Chaos and Quantum Physics,* 1989 Les Houches Lectures, edited by M. J. Giannoni, A. Voros, and J. Zinn-Justin (North-Holland, Amsterdam, 1991).
[2] *Chaos and Quantum Chaos,* edited by W. D. Heiss, Lecture Notes in Physics Vol. 411 (Springer, Berlin, 1992).
[3] A. J. Lichtenberg, M. A. Liebermann, *Regular and Stochastic Motion* (Springer, New York, 1983).
[4] J. Ford, in *Directions in Chaos,* edited by B.-L. Hao (World Scientific, Singapore, 1988), p. 128.
[5] B. V. Chirikov, in *Chaos and Quantum Chaos* (Ref. [2]), p. 1.
[6] J. Ford and G. Mantica, Am. J. Phys. **60**, 1086 (1992).
[7] G. Casati, B. V. Chirkikov, F. M. Izraelev, and J. Ford, in *Stochastic Behavior in Classical and Quantum Hamiltonian Systems,* edited by G. Casati and J. Ford, Lecture Notes in Physics Vol. 93 (Springer, Berlin, 1979), p. 334.
[8] H. Frahm and H. J. Mikeska, Z. Phys. B **60**, 117 (1985).
[9] T. Hogg, and B. A. Hubermann, Phys. Rev. A **28**, 22 (1983).
[10] J. Ford and M. Ilg, Phys. Rev. A **45**, 6165 (1992).
[11] D. L. Shepelyansky, Physica D **8**, 208 (1983).
[12] J. Bellissard, in *Stochastic Processes in Classical and Quantum Systems,* edited by S. Albeverio, G. Casati, and D. Merlini, Lecture Notes in Physics Vol. 262 (Springer, Berlin, 1985), p. 24.
[13] M. V. Berry, Physica D **10**, 369 (1984).
[14] V. I. Arnold and A. Avez, *Ergodic Problems of Classical Mechanics* (Benjamin, Reading, MA, 1968).
[15] M. V. Berry, M. L. Balazs, M. Tabor, and A. Voros, Ann. Phys. (N.Y.) **122**, 26 (1979).
[16] J. Ford, G. Mantica, and G. Ristow, Physica D **50**, 493 (1991).
[17] St. Weigert, Z. Phys. B **80**, 3 (1990).
[18] B. V. Chirikov, F. M. Izrailev, and D. L. Shepelyansky, Physica D **33**, 77 (1988).
[19] M. V. Berry, in *Dynamics and Patterns in Complex Fluids,* edited by A. Onuki and K. Kawasaki (Springer, Berlin, 1990), p. 123.
[20] V. M. Alekseev, and M. V. Yakobson, Phys. Rep. **75**, 287 (1981).
[21] G. J. Chaitin, *Algorithmic Information Theory* (Cambridge University Press, Cambridge, 1987).
[22] G. J. Chaitin, *Information, Randomness and Incompleteness* (World Scientific, Singapore, 1987).
[23] B. Eckhardt, J. Ford, and F. Vivaldi, Physica D **13**, 339 (1984).
[24] J. Moser, *Stable and Random Motions in Dynamical Systems* (Princeton University Press, Princeton, 1973), Vol. 77
[25] H. R. Grümm, H. Narnhofer, and W. Thirring, Act. Phys. Austr. **57**, 175 (1985).
[26] G. Casati, L. Molinari, Prog. Theor. Phys. Suppl. **98**, 287 (1989).
[27] J. Ford, in *Chaotic Dynamics and Fractals,* edited by M. F. Barnsley and St. G. Demko (Academic, New York, 1986).
[28] St. Weigert, Phys. Rev. A **43**, 6597 (1991).
[29] R. Blümel, and U. Smilansky, Phys. World **2**, 30 (1990).
[30] T. Geisel, Phys. Rev. A **41**, 2989 (1990).
[31] O. Bohigas, M. J. Giannoni, and C. Schmit, J. Phys. Lett. **45**, L1015 (1984).
[32] J. H. Jensen, in *Quantum Chaos,* edited by H. A. Cerdeira, R. Ramaswamy, M. C. Gutzwiller, and G. Casati (World Scientific, Singapore, 1991), p. 111.
[33] G. A. Luna-Acosta, in *Quantum Chaos* (Ref. [33]), p. 118.
[34] R. V. Mendes, J. Phys. A **24**, 4349 (1991).
[35] R. V. Mendes, Phys. Lett. A **171**, 253 (1992).
[36] M. Toda, S. Adachi, and K. Ikeda, Prog. Theor. Phys. **98**, 323 (1989).
[37] E. Fick, *Einführung in die Grundlagen der Quantentheorie* (Akademische Verlagsgesellschaft, Frankfurt, 1972).
[38] MACSYMA symbolic programming package reference manual, Symbolics, Inc., Burlington, 1988.